European Journal of Medicinal Chemistry 259 (2023) 115561

Contents lists available at ScienceDirect

European Journal of Medicinal Chemistry

journal homepage: www.elsevier.com/locate/ejmech

Research paper

Immunosuppressive effects of new thiophene-based $K_V1.3$ inhibitors

Špela Gubič [a], Alberto Montalbano [b], Cesare Sala [b], Andrea Becchetti [c], Louise Antonia Hendrickx [d], Kenny M. Van Theemsche [e,f], Ernesto Lopes Pinheiro-Junior [d], Ginevra Chioccioli Altadonna [g], Steve Peigneur [d], Janez Ilaš [a], Alain J. Labro [f], Luis A. Pardo [h], Jan Tytgat [d], Tihomir Tomašič [a], Annarosa Arcangeli [b,**], Lucija Peterlin Mašič [a,*]

[a] University of Ljubljana, Faculty of Pharmacy, Department of Pharmaceutical Chemistry, Aškerčeva cesta 7, 1000, Ljubljana, Slovenia
[b] University of Florence, Department of Experimental and Clinical Medicine, I-50134, Florence, Italy
[c] University of Milano-Bicocca, Department of Biotechnology and Biosciences, Piazza della Scienza 2, I-20126, Milano, Italy
[d] University of Leuven, Toxicology and Pharmacology, Campus Gasthuisberg, Onderwijs en Navorsing 2, Herestraat 49, PO Box 922, 3000, Leuven, Belgium
[e] University of Antwerp, Department of Biomedical Sciences, Campus Drie Eiken, Universiteisplein 1, 2610, Wilrijk, Belgium
[f] Ghent University, Department of Basic and Applied Medical Sciences, Corneel Heymanslaan 10, 9000, Ghent, Belgium
[g] University of Siena, Department of Medical Biotechnologies, I-53100, Siena, Italy
[h] Max-Planck Institute for Experimental Medicine, AG Oncophysiology, Hermann-Rein-Str. 3, 37075, Göttingen, Germany

ARTICLE INFO

Keywords:
Ion channel
$K_V1.3$ inhibitor
T-lymphocyte
Immunosuppressive

ABSTRACT

Voltage-gated potassium channel $K_V1.3$ inhibitors have been shown to be effective in preventing T-cell proliferation and activation by affecting intracellular Ca^{2+} homeostasis. Here, we present the structure-activity relationship, $K_V1.3$ inhibition, and immunosuppressive effects of new thiophene-based $K_V1.3$ inhibitors with nanomolar potency on K^+ current in T-lymphocytes and $K_V1.3$ inhibition on Ltk^- cells. The new $K_V1.3$ inhibitor *trans*-**18** inhibited $K_V1.3$ -mediated current in phytohemagglutinin (PHA)-activated T-lymphocytes with an IC_{50} value of 26.1 nM and in mammalian Ltk^- cells with an IC_{50} value of 230 nM. The $K_V1.3$ inhibitor *trans*-**18** also had nanomolar potency against $K_V1.3$ in *Xenopus laevis* oocytes (IC_{50} = 136 nM). The novel thiophene-based $K_V1.3$ inhibitors impaired intracellular Ca^{2+} signaling as well as T-cell activation, proliferation, and colony formation.

1. Introduction

The voltage-gated potassium channel $K_V1.3$ and the calcium-activated potassium channel $K_{Ca}3.1$ are the most prevalent and best characterized potassium channels expressed by human T-lymphocytes, with $K_V1.3$ preferentially upregulated over $K_{Ca}3.1$. These channels provide the K^+ efflux and resulting negative values of the resting plasma membrane potential required for adequate Ca^{2+} influx that is critical for T-cell activation. At rest, T-lymphocytes express only low levels of $K_V1.3$ and $K_{Ca}3.1$ channels, however, both are upregulated upon antigen- or mitogen-specific activation. Their dysregulation may therefore be related to abnormal lymphocyte activation [1–5].

$K_V1.3$, a homotetramer composed of individual α-subunits, each consisting of six transmembrane segments, is activated by membrane depolarization [6]. Charged S4 segment constitutes the main part of the voltage sensor which senses membrane voltage, resulting in a conformational change that causes channel opening [7]. $K_{Ca}3.1$ is a calcium-activated potassium channel whose carboxy terminus is bound to calmodulin, which controls channel opening [8]. Therefore, this channel induces membrane repolarization after Ca^{2+} entry. Electrophysiological studies have indicated that $K_V1.3$ plays a critical role in regulating chronically activated effector memory T-cell (T_{EM}) immune responses [9]. The role of $K_V1.3$ and $K_{Ca}3.1$ in calcium signaling is controlled by their expression levels, which vary during different phases of lymphocyte development, subsets, and activation state [2,10–12]. When naïve and central memory T-cells (T_{CM}) are activated, they upregulate the expression of $K_{Ca}3.1$ per cell but maintain stable $K_V1.3$ expression. Conversely, T_{EM} increases $K_V1.3$ expression upon activation, while keeping the concentration of $K_{Ca}3.1$ per cell constant. Given the prominent role that the $K_V1.3$ channel plays in lymphocyte

* Corresponding author. University of Ljubljana, Faculty of Pharmacy, Aškerčeva cesta 7, 1000, Ljubljana, Slovenia.
** Corresponding author.
E-mail addresses: annarosa.arcangeli@unifi.it (A. Arcangeli), lucija.peterlinmasic@ffa.uni-lj.si (L. Peterlin Mašič).

https://doi.org/10.1016/j.ejmech.2023.115561
Received 19 January 2023; Received in revised form 8 June 2023; Accepted 8 June 2023
Available online 25 June 2023

development, activation, and selection, it has become an important prognostic and drug target [13–16]. In addition, the finding that $K_V1.3$ and $K_{Ca}3.1$ activate distinct lymphocyte subsets offers the possibility of targeting lymphocyte subsets more specifically for therapeutic purposes [13].

$K_V1.3$ inhibitors can selectively target the disease-causing T_{EM} population without affecting the other immune cells, and therefore have implications for all T-cell-mediated autoimmune and chronic inflammatory diseases such as psoriasis, multiple sclerosis, type 1 diabetes mellitus, atherosclerosis, asthma, and rheumatoid arthritis [17]. Depolarization of membranes by $K_V1.3$ inhibition has been shown to be effective in preventing T-cell proliferation and terminating cytokine production [18].

Some of the small molecule $K_V1.3$ inhibitors (Fig. 1) have been developed to inhibit $K_V1.3$ in the plasma membrane of T_{EM} cells and induce an immunosuppressive response by regulating intracellular Ca^{2+} homeostasis [18]. The major challenge in developing small molecule $K_V1.3$ inhibitors is isoform selectivity, as $K_V1.x$ family channels exhibit high subtype homology [19]. The psoralen analog PAP-1 (**1**, Fig. 1) inhibited native $K_V1.3$ channels in human T-lymphocytes with an IC_{50} value of 2.1 nM and cloned $K_V1.3$ channels in L929 cells with an IC_{50} value of 2.0 nM. It was 23-fold more selective for $K_V1.3$ than over cardiac $K_V1.5$ channels and was 33- to 125-fold selective over other $K_V1.x$ family channels [20]. PAP-1 (**1**) dose-dependently inhibited interleukin 2 (IL-2) and interferon-γ production in vitro. It also improved pathology in the mouse psoriasis skin xenograft model of severe combined immunodeficiency (SCID). Its efficacy was demonstrated in female Lewis rats, where it suppressed the delayed hypersensitivity response in a dose-dependent manner [21]. The compound PAP-1 is practically insoluble in water (aqueous solubility <1 mg/mL) [22]. Its hydroxyl analog (PAP-OH) has a solubility of 0.6 ± 0.1 μM (aqueous solution DMEM). Adding six monomeric ethylene glycol units to the phenyl ring of PAP-1 increases the solubility to 30 ± 3 μM (aqueous solution DMEM) (PAP-1-MHEG) [23].

Compound Psora-4 (**2**, Fig. 1) is another potent psoralen-based $K_V1.3$ inhibitor with a low nanomolar potency for $K_V1.3$, as determined by two independent assay systems [24]. It suppressed the proliferation of human and rat myelin-specific effector memory T-cells. This psoralen analog showed 17- to 70-fold selectivity for $K_V1.3$ over closely related $K_V1.x$ family channels ($K_V1.1$, $K_V1.2$, $K_V1.4$, and $K_V1.7$), with the exception of $K_V1.5$ (IC_{50} = 7.7 nM), and is therefore a less selective $K_V1.3$ inhibitor compared to PAP-1 [24].

The benzamide compound PAC (**3**, Fig. 1) was identified as a nanomolar $K_V1.3$ inhibitor in Merck's high-throughput screening campaign using the ^{86}Rb flux assay and also inhibited native $K_V1.3$ currents in human T-lymphocytes. However, compound PAC lacked selectivity toward other $K_V1.x$ family channels [25]. Its carbamate analogs (*trans*-**4** and *cis*-**4**, Fig. 1) inhibited $K_V1.3$ currents even more strongly in flux assays. The *trans*-benzamide isomers showed low selectivity for $K_V1.3$ over the other $K_V1.x$ family channels. *In vitro* functional assays showed that benzamides **3**, *trans*-**4**, and *cis*-**4** reversibly inhibited Ca^{2+}-dependent activation of T-lymphocytes. $K_V1.3$ inhibitors **3** and *trans*-**4** induced concentration-dependent [^{3}H]thymidine uptake in human T-cells with IC_{50} values of 1 μM and 340 nM, respectively [25].

Because the binding site of psoralen- and benzamide-based $K_V1.3$ inhibitors is unknown, we used a ligand-based drug design approach based on a 3D similarity search of previously published benzamide inhibitors (Fig. 1) and found a novel thiophene-based hit, compound **5** (Fig. 1), that is selective for $K_V1.3$ channels [26]. Structural modification of compound **5** gave us the 3-thiophene-based $K_V1.3$ inhibitor **6** with an IC_{50} value of 470 nM and 18-fold selectivity over closely related $K_V1.x$ family channels in the *Xenopus laevis* oocytes (Fig. 2) [27]. Here, we report the investigation of the structure-activity relationship of new thiophene-based $K_V1.3$ inhibitors, the inhibition of $K_V1.3$ channels in T-lymphocytes, Ltk^- cells, and *Xenopus laevis* oocytes, and the effects of structural changes on thermodynamic solubility. The most potent thiophene-based $K_V1.3$ inhibitors were tested for their selectivity and immunosuppressive effects with PHA-activated T-cells from peripheral blood mononuclear cells (PBMCs). The new $K_V1.3$ inhibitors impaired intracellular Ca^{2+} signaling and T-cell activation, proliferation, and colony formation.

2. Results and discusion

2.1. Structure-activity relationship study and synthesis of new thiophene-based $K_V1.3$ inhibitors

We performed a structure-activity relationship study of the hit compound **6** to increase its potency on $hK_V1.3$ inhibition (Fig. 2). We designed type I and type II compounds based on 2-thiophene and 3-thiophene scaffolds, respectively. In a 2-thiophene type I series, we modified both the tetrahydropyran and 2-methoxyphenyl moieties of compound **6**. The tetrahydropyran ring was replaced by an oxo, hydroxyl and carbamate substituted cyclohexane ring. In the oxo compounds, we substituted the 2-methoxyphenyl moiety of compound **14** with 5-methyl (**7**), 5-fluoro (**8**) and 4-methyl (**10**) substituents. In addition, 2-methoxyphenyl moiety of compound **14** was changed with the 3-furanyl moiety (compound **9**). All hydroxyl- and carbamate-substituted diasteroisomeric mixtures were separated into their *cis*- and *trans*-isomers by column chromatography. In the hydroxyl series, the 2-methoxyphenyl

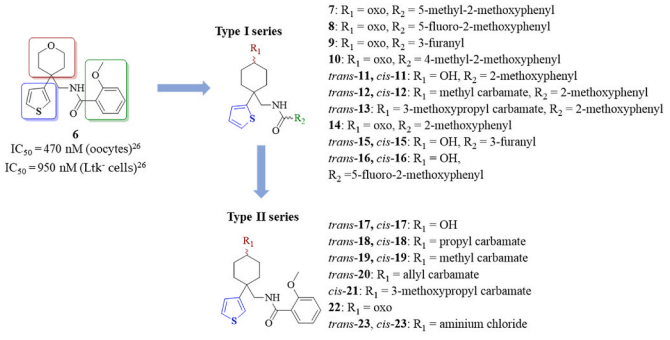

Fig. 2. Design of new thiophene-based $K_V1.3$ inhibitors.

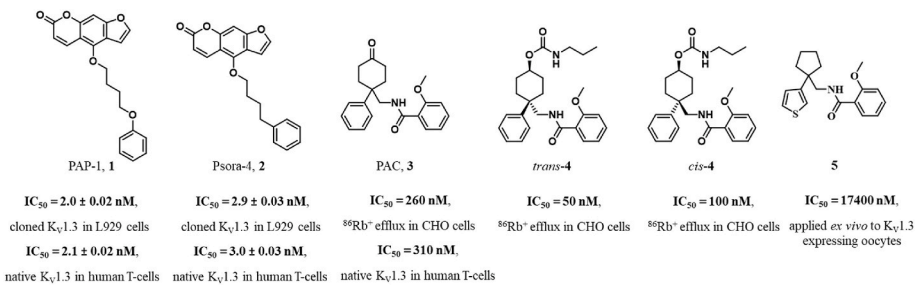

Fig. 1. Examples of known $K_V1.3$ inhibitors [20,24,25].

moiety of compounds *cis*- and *trans*- **11** was changed for 3-furanyl (*cis*- and *trans*- **15**) and 5-fluoro-2-metoxyphenyl (*cis*- and *trans*- **16**) moieties. The hydroxyl compound **11** was also substituted with methyl carbamate (*cis*- and *trans*- **12**) and 3-methoxypropyl carbamate (*trans*-13) moieties. Based on the type I series results, we optimized only the tetrahydropyran moiety in the II 3-thiophene series, as we found that 2-metoxyphenyl was optimal at this position. In the 3-thiophene series the hydroxyl group (compounds *cis*- and *trans*- **17**) was substituted with different carbamates: methyl (*cis*- and *trans*- **19**), propyl (*cis*- and *trans*- **18**), allyl (*cis*- and *trans*- **20**) and 3-methoxypropyl (*cis*- and *trans*- **22**). In addition, the hydroxyl group of compounds *cis*- and *trans*- **17** was changed for the amino group (*cis*- and *trans*- **23**). These modifications allowed us to increase the potency for $K_V1.3$ inhibition and to investigate the effects of the structural changes on TD solubility.

The synthesis of the new type I and II compounds **7**–**23** is shown in Schemes 1–3. The thiophene-2-acetonitrile or thiophene-3-acetonitrile (Scheme 1) were converted to the 4,4-disubstituted-2-carbomethoxycyclohexanone intermediates **24** and **25** by an efficient two-pot synthetic method. First, thiophene-2-acetonitrile or thiophene-3-acetonitrile were refluxed in *tert*-butanol to react in a double Michael addition in the presence of methyl acrylate and benzyl trimethylammonium hydroxide (Triton B) to give diester intermediates (not shown). Subsequently, the intermediates were deprotonated in a separate step with potassium *tert*-butoxide to afford the 4-heteroaryl-4-cyano-2-carbomethoxycyclohexanone derivatives **24** and **25** (Scheme 1) by Dieckmann condensation. The 2-carboxymethyl group was then removed to give the corresponding 4-cyano-4-heteroarylcyclohexanone derivatives **26** and **27** (Scheme 1) by stirring at 100 °C in a mixture of 10% sulfuric acid and glacial acetic acid. The ketone group was protected with ethylene glycol to give the intermediates **28** and **29** (Scheme 1). Reduction of the carbonitrile group in the presence of $LiAlH_4$ in tetrahydrofuran (THF) yielded the primary amines **30** and **31**, which were then reacted with 2-methoxybenzoyl chloride to give the intermediates **32** and **33** (Scheme 1). The protecting group was then removed to give ketones **7**, **8**, **9**, **10**, **14** and **22** (Scheme 1 and Scheme 2). The ketone group was selectively reduced in the presence of $NaBH_4$ to yield a diasteroisomeric mixture of alcohols **11**, **15**, **16**, and **17** (Scheme 1 and Scheme 2), which were separated to their *cis*- and *trans*-isomers by column chromatography. The hydroxy analogs were then reacted with 4-nitrochloroformates (Scheme 2 and Scheme 3) to afford 4-nitrophenyl carbonate intermediates, which were reacted with various primary amines to give the new carbamate derivatives *trans*-**12**, *cis*-**12**, *trans*-**13**, *trans*-**18**, *cis*-**18**, *trans*-**19**, *cis*-**19**, *trans*-**20**, and *cis*-**21**. The amines *trans*-**23** and *cis*-**23** were obtained from the alcohol intermediates *trans*-**17** and *cis*-**17** via a four-step procedure: mesylation of the hydroxyl group with methanesulfonyl chloride (MsCl), nucleophilic substitution of the mesylate with azide, reduction of the azide to the amine with catalytic hydrogenation, and formation of the hydrochloride salt with 4 M HCl in 1,4-dioxane (Scheme 3).

2.2. $K_V1.3$ inhibitory potencies on *Xenopus laevis* oocytes and Ltk^- cells

All new type I and type II compounds were first screened for their $K_V1.3$ inhibition in *Xenopus laevis* oocytes expressing human $hK_V1.3$ (Table 1). Compounds that exhibited more than 90% reduction in total outward potassium current at 10 μM were tested for their $hK_V1.3$ inhibition in mouse fibroblast Ltk^- cells using manual patch-clamp

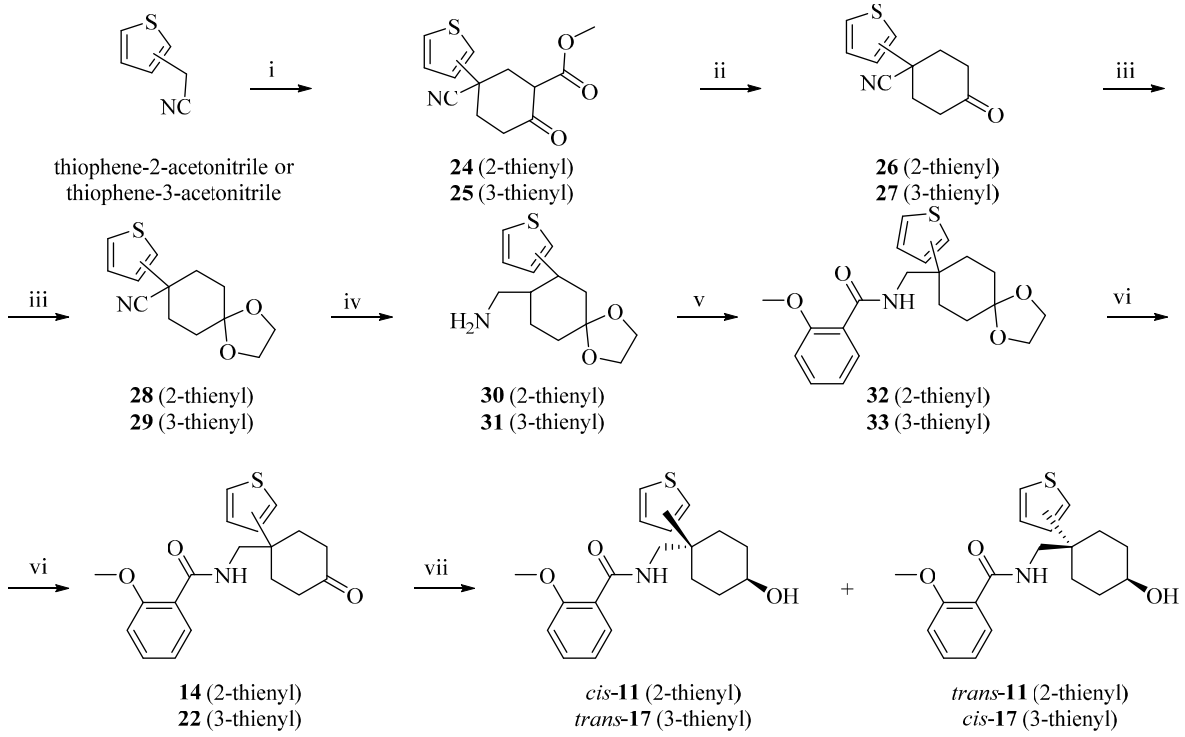

Scheme 1. Synthesis of hydroxyl- and oxo-based 3-thiophene and 2-thiophene $K_V1.3$ inhibitors[a].

[a] Reagents and conditions: (i) (a) methyl acrylate, benzyltrimethylammonium hydroxide, *tert*-butanol, reflux, 4 h (80–81%); (b) potassium *tert*-butoxide, anhydrous THF, 0 °C, reflux, 5 h, room temperature (rt), overnight (60–77%); (ii) 10% sulfuric acid, glacial acetic acid, 100 °C, 24 h (50–62%); (iii) ethane-1,2-diol, *p*-toluenesulfonic acid (PTSA), toluene, 140 °C, overnight (96–98%); (iv) $LiAlH_4$, anhydrous THF, 0 °C, rt, overnight (96–97%); (v) (a) appropriate benzoic acid, oxalyl chloride, dichloromethane (DCM), 2 drops *N,N*-dimethylformamide (DMF), rt, overnight (100%); (b) 2-methoxybenzoyl chloride or appropriate benzoyl chloride, Et_3N, DCM, rt, overnight (89–95%); (vi) water, pyridinium *p*-toluenesulfonate, acetone, reflux, overnight (75%); (vii) sodium borohydride, anhydrous THF, 0 °C, rt, overnight (*trans* 34–43% and *cis* 31–57%).

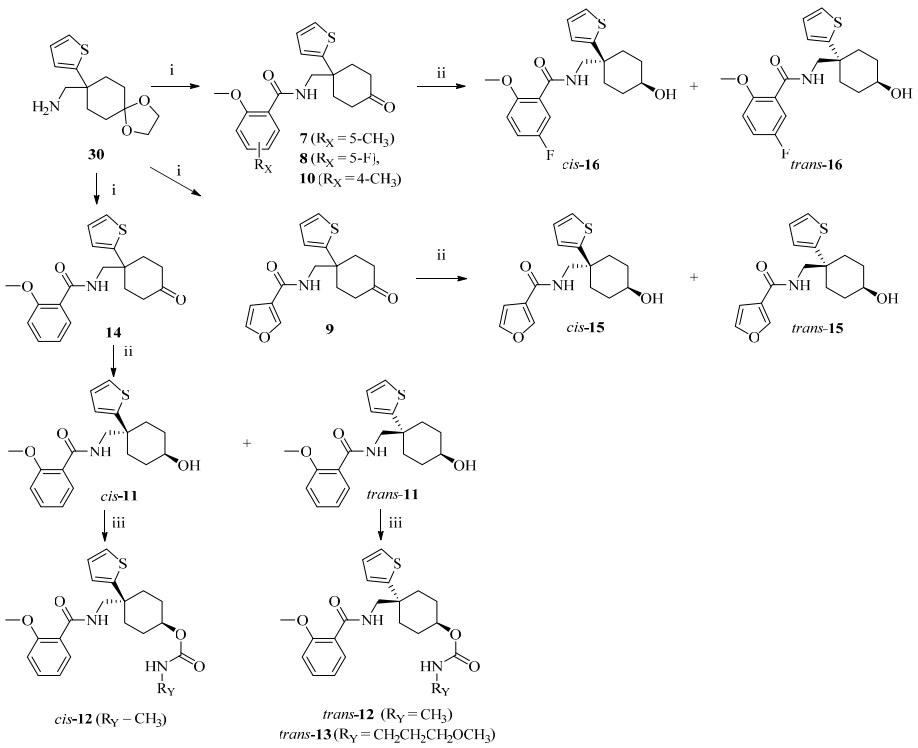

Scheme 2. Synthesis of new alcohol and carbamate derivatives of 2-thiophene-based $K_V1.3$ inhibitors[a].
[a] Reagents and conditions: (i) (a) 2-methoxybenzoic acid or furan-3-carboxylic acid or appropriate benzoic acid, oxalyl chloride, DCM, 2 drops DMF, rt, overnight (100%); (b) 2-methoxybenzoyl chloride or furan-3-carbonyl chloride or appropriate benzoyl chloride, Et_3N, DCM, rt, overnight (57–96%); (3) water, pyridinium *p*-toluenesulfonate, acetone, reflux, overnight (46–75%); (ii) sodium borohydride, anhydrous THF, 0 °C, rt, overnight (*cis* 16–34% and *trans* 24–43%); (iii) (a) 4-nitrophenyl chloroformate, Et_3N, DCM, rt, overnight (52%); (b) methyl amine or other appropriate amine, DCM, rt, overnight (85–92%).

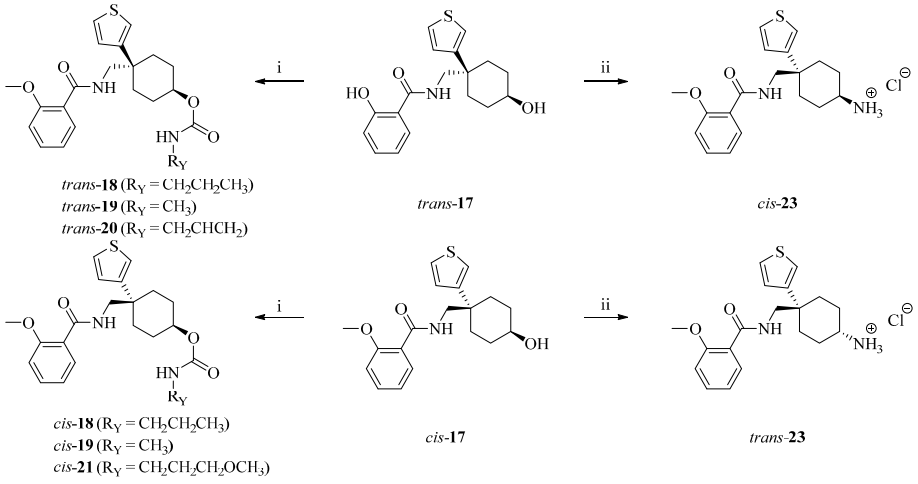

Scheme 3. Synthesis of carbamate derivatives of 3-thiophene-based $K_V1.3$ inhibitors[a].
[a] Reagents and conditions: (i) (a) 4-nitrophenyl chloroformate, Et_3N, DCM, rt, overnight (52%); (b) appropriate amine, DCM, rt, overnight (81–96%); (ii) (a) methanesulfonyl chloride, Et_3N, DCM, ice bath, 2 h (100%); (b) sodium azide, DMF, 100 °C, overnight (50–57%); (c) $H_{2(g)}$, Pd/C, methanol (MeOH), rt, overnight (86%); (d) 4 M HCl in 1,4-dioxane, MeOH, rt, 1 h (34–42%).

technique to demonstrate inhibition of $hK_V1.3$ in a mammalian cell line and to determine dose-response relationships (Table 2, Fig. S1 and Fig. S2) (see Table 3).

From the results in Table 1, the preferred moiety in the R_2 position is 2-methoxyphenyl. For the type I compounds, the potency was maintained when the cyclopyran ring (starting compound **6**) was replaced by cyclohexanone (compound **14**). Further conversion of the ketone (**14**) to a hydroxyl analogue (**11**) resulted in increased potency, with the *trans*-**11** analogue being more potent than the *cis*-**11** analogue. Among the carbamates, the methyl carbamate **12** was the most potent and in this case the *cis* isomer was more potent compared to the *trans* isomer with IC_{50} values of 470 and 180 nM, respectively. In the II series with the 3-tiophene and 2-methoxyphenyl moieties, the same trends were observed, with the hydroxyl compound (**17**) being more potent than the ketone compound (**22**) and, among the carbamates, the methyl carbamate (*trans*-**19**) and propyl carbamate (*trans*-**18**) being the most potent with IC_{50} values of 170 and 230 nM, respectively. The optimization strategy resulted in increased potency of parent compound **6** for human $hK_V1.3$ channels expressed in Ltk cells and in *Xenopus laevis* oocytes.

2.3. Inhibition of $K_V1.3$ -mediated current on PHA-activated T-lymphocytes

There is growing evidence of the critical role that potassium channels

Table 1
$K_V1.3$ inhibitory potencies in *Xenopus laevis* oocytes of reference compounds **3**–**4**, and of the newly designed Type I (**7**–**16**) and Type II (**17**–**23**) analogs, manually patch-clamped to determine the percentage of inhibition at 10 μM.

Compound ID	% of $K_V1.3$ inhibition at 10 μM	Compound ID	% of $K_V1.3$ inhibition at 10 μM
3	87.48 ± 6.27%	*trans*-**15**	65.70 ± 10.39%
trans-**4**	87.30 ± 6.47%	*cis*-**16**	54.87 ± 6.50%
cis-**4**	40.50 ± 9.47%	*trans*-**16**	66.44 ± 3.92%
7	23.28 ± 5.27%	*trans*-**17**	78.53 ± 7.11%
8	39.11 ± 4.51%	*cis*-**17**	**97.63 ± 0.85%**
9	55.31 ± 5.99%	*trans*-**18**	**90.67 ± 4.33%**
10	85.59 ± 4.61%	*cis*-**18**	25.53 ± 6.35%
cis-**11**	38.52 ± 6.24%	*trans*-**19**	**93.04 ± 1.77%**
trans-**11**	**90.93 ± 3.07%**	*cis*-**19**	79.62 ± 4.92%
trans-**12**	**93.75 ± 1.58%**	*trans*-**20**	36.16 ± 11.88%
cis-**12**	**94.71 ± 1.74%**	*cis*-**21**	**94.45 ± 1.22%**
trans-**13**	**91.61 ± 4.22%**	**22**	**97.01 ± 1.13%**
14	**95.06 ± 0.98%**	*trans*-**23**	0.65 ± 5.60%
cis-**15**	0 ± 0.85%	*cis*-**23**	6.46 ± 11.77%

Table 2
IC_{50} values determined on $hK_V1.3$ channels expressed in Ltk^- cells.

compound ID	structural type	IC_{50} [nM] Ltk^- cells
6	reference	950 ± 240
trans-**11**	type I	250 ± 20
trans-**12**	type I	470 ± 10
cis-**12**	type I	180 ± 10
trans-**13**	type I	850 ± 60
14	type I	1130 ± 10
cis-**17**	type II	450 ± 10
trans-**18**	type II	230 ± 10
trans-**19**	type II	170 ± 10
cis-**21**	type II	670 ± 20
22	type II	800 ± 20

Table 3
IC_{50} values of selected thiophene-based $K_V1.3$ inhibitors on PHA-activated T-lymphocytes.

Compound ID	Structural type	IC_{50} [nM] PHA-activated T-lymphocytes
cis-**17**	type II	56.83 ± 0.08
trans-**18**	type II	26.12 ± 0.09
trans-**20**	type II	37.21 ± 0.07

play in cellular mechanisms that regulate cell cycle progression, selection, differentiation, and migration of cells under both physiological and pathological conditions, such as tumors [18,28,29]. These findings are more relevant in T-lymphocytes because the ability of these cells to increase functional expression of $K_V1.3$ channels upon stimulation by the T-cell receptor (TCR) has already been demonstrated [30–32]. In this study, we optimized the PBMC isolation method to use PHA-activated T-lymphocytes as a target for electrophysiological studies of potassium currents mediated by $K_V1.3$ channels. PBMCs were analyzed after 5 days of PHA stimulation, and almost all (~90%) of the cells were $CD3^+$ T-lymphocytes.

First, we examined the functional presence of $K_V1.3$ channels in PBMC PHA-activated T-lymphocytes using the inhibitor Psora-4 (1 μM, 1 min application, Figs. S3A and S3B). Under control conditions, an average outward current of 1187 ± 387.2 pA (n = 7) was measured. The measured outward current in the presence of Psora-4 (1 μM, 1 min application was reduced on average to 60.5 ± 43.8 pA (96% reduction, n = 7, p < 0.001, paired *t*-test). Previously, the calculated Psora-4-sensitive current averaged 1126 ± 375.2 pA. Our data showed a significant 96% reduction in potassium current after Psora-4 application (1 μM, 1 min administration, Fig. S3B).

We next wanted to investigate whether the residual outward current observed after Psora-4 application was due to the presence of a $K_{Ca}3.1$ current, since it is known from the literature that these cells also express functional $K_{Ca}3.1$ channels [30]. To this end, we repeated the two-step protocol previously described to evoke potassium outward currents under control conditions and in the presence of the specific inhibitor for $K_{Ca}3.1$ channels TRAM-34 [33]. The outward current measured under control conditions averaged 769.2 ± 199.2 pA, whereas in the presence of TRAM-34 (1 μM, 1 min application) it was reduced to an average of 596.3 ± 163.5 pA (18% reduction, n = 6, p = 0.519, paired *t*-test) such that the TRAM-34-sensitive net current averaged 173.0 ± 149.9 pA (Figs. S3C and S3D). These data, obtained using the specific blocker for $K_{Ca}3.1$ TRAM-34 (1 μM), showed that the potassium current component mediated by these channels was small and negligible (18% nonsignificant reduction).

Therefore, in agreement with the observations of other authors [29–31], PHA-mediated activation of T-lymphocytes resulted in successful overexpression of $K_V1.3$ channels also in our case. Considering the negligible contribution of $K_{Ca}3.1$, PBMC-derived T-lymphocytes stimulated with PHA represent an excellent tool to study $K_V1.3$ channels without the need to use cellular transfection methods, which are certainly more invasive and therefore far from physiological conditions.

We resynthesized Merck benzamide inhibitors **3**, *trans*-**4**, and *cis*-**4** according to Scheme S1 and the procedures described previously and tested them on PHA-activated T-lymphocytes [27]. All three phenyl-based Merck benzamides (reference compounds **3**, *trans*-**4**, and *cis*-**4**) showed functional inhibition of $K_V1.3$ channels but were less potent in inhibiting channel currents than our 3-thiophene-based benzamide reference **6** in the same assay at 5 μM (Fig. 3, blue columns).

The new type I (orange) and type II (green) analogs **7**–**23** showed functional activity as inhibitors of $K_V1.3$ channels and were able to induce a significant reduction in the total outward potassium current at a concentration of 5 μM, although to different extents (Fig. 3, Table S1). The new type II 3-thiophene-based analogs *trans*-**18** (propyl carbamate analog) and *cis*-**17** (hydroxyl analog) showed the most pronounced effects among all the compounds tested. The type II *trans*-carbamates (*trans*-**18**, *trans*-**19**, and *trans*-**20**) showed a greater reduction in total outward potassium current than the *cis*-carbamates (*cis*-**18**, *cis*-**19**, and *cis*-**21**) at a concentration of 5 μM. Conversely, the type II *cis*-alcohol (*cis*-**17**) caused a higher percentage of $K_V1.3$ inhibition than the *trans*-alcohol compound (*trans*-**17**), which was consistently observed in *Xenopus laevis* oocytes and Ltk^- cells (Table 2). The type II ketone compound **22** and the amines *trans*-**23** and *cis*-**23** showed a lower percentage of channel inhibition than the most potent alcohol *cis*-**17** and the

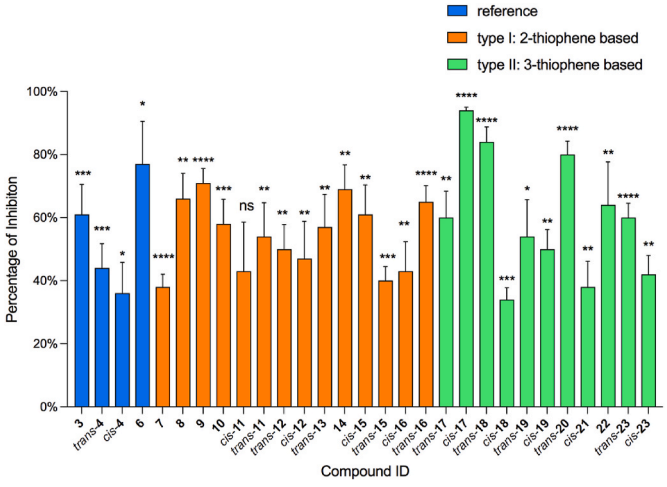

Fig. 3. Percentages of inhibition produced by the application of reference compounds (blue), type-I 2-thiophene based compounds (orange) and type-II 3-thiophene based compounds (green) on PBMC PHA-activated T-lymphocytes at 5 μM. ns = not significant.

carbamates *trans*-**18** and *trans*-**20**. The potency of the starting compound **6** on PBMC PHA-activated T-lymphocytes was improved by modifying the tetrahydropyran moiety with the hydroxyl (*cis*-**17**) and carbamate (*trans*-**18**) substituted cyclohexane-based compounds. Of the type I compounds (Fig. 3, Table S2), the most potent inhibition of total current was caused by ketones **8**, **9**, and **14**, which were, however, significantly less potent than the most potent type II compounds (*cis*-**17**, *trans*-**18**, and *trans*-**20**). The type I ketones (**7**, **8**, **9**, and **10**) contained modifications of the 2-methoxybenzamide moiety, and the tolerated substitutions were 5-fluoro-2-methoxybenzamide (**8**), furan-3-carboxamide (**9**), and 4-methyl-2-methoxybenzamide (**10**), but the substitution of 5-methyl-2-methoxybenzamide (**7**) significantly reduced the inhibitory effect.

To characterize the pharmacological activity of the most potent new $K_V1.3$ inhibitors *cis*-**17**, *trans*-**18**, and *trans*-**20**, which showed the highest percentage of inhibition at 5 μM (Fig. 3), dose-response assays were performed (Fig. S4) and representative current traces currents of PBMC-derived PHA-activated T-lymphocytes in the presence of *cis*-**17** and *trans*-**18** were added in the Supplementary Fig. S5. The new type II 3-thiophene-based analogs *cis*-**17**, *trans*-**18**, and *trans*-**20** (Table 1) had nanomolar potencies on human PBMC PHA-activated T-lymphocytes. Compound *trans*-**18** was the most potent, with an IC_{50} value of 26.1 nM.

Based on $K_V1.3$ -mediated current inhibition assays on PHA-activated T-lymphocytes and $K_V1.3$ inhibition effects on Ltk^- cells, we obtained the new promising $K_V1.3$ inhibitor *trans*-**18** with nanomolar potencies on human PBMC PHA-activated T-lymphocytes (IC_{50} = 26.1 nM) and mammalian Ltk^- cells (IC_{50} = 230 nM). Therefore, we also tested *trans*-**18** against similar voltage-gated potassium channels $K_V1.1$-$K_V1.6$ using the *Xenopus laevis* heterologous expression system. The propyl carbamate analog *trans*-**18** also had nanomolar potency against $K_V1.3$ in *Xenopus laevis* oocytes (IC_{50} = 135.6 ± 5.2 nM) and was selective against $K_V1.4$, $K_V1.5$, and $K_V1.6$ channels (% inhibition = 6.4 ± 6.9%, 11.4 ± 7.3%, and −1.1 ± 4.0%, respectively), but no selectivity towards $K_V1.1$ (Fig. S6, IC_{50} = 124.1 ± 0.9 nM) and $K_V1.2$-channels (Fig. S6, IC_{50} = 308.0 ± 18.1 nM). In terms of thermodynamic solubility (TD), the most soluble compounds in a series were ketones **14** and **22** with TD solubilities of 210 μM and 400 μM, respectively (Table S2). The compound *trans*-**18** is stable in the PBS buffer (pH = 7.4) for at least 120 h (Fig. S7). The most promising compounds on human PBMC PHA-activated T-lymphocytes and mammalian Ltk^- cells had TD solubilities of 72 μM (*cis*-**17**) and 22 μM (*trans*-**18**), which were higher than that of PAP-1. In addition, HEK-293 model cells were used to overexpress the hERG potassium channel and test the hERG inhibition of selected new thiophene-based $K_V1.3$ inhibitors. Each of these inhibitors showed current reduction of 21% (*cis*-**15**), 15% (*cis*-**17**), 21% (*trans*-**18**), and 19% (*trans*-**19**) at 5 μM (Fig. S8).

Comparing the response of Kv1.3-mediated currents to *trans*-**18** in heterologous expression systems with PHA-activated T-lymphocytes, approximately a 10-fold higher affinity was observed in the latter. Ltk-cells are known to express the Kvbeta2.1 subunit that might affect the drug response of Kv1.3 [34]. On the other hand, it is reported that a Kvbeta2 subunit is also expressed in T lymphocytes [35]. Therefore, we do not expect that the difference can be ascribed to the presence of this auxiliary Kvbeta2.1 subunit in Ltk-cells. The obtained IC_{50} value in the Kv1.3 expressing Ltk-cells was less than a 2-fold difference from the one obtained in Xenopus oocytes. Possibly for these compounds it is the absence of other subunits or specific lipid composition (microdomains) present in the T lymphocytes that increases the affinity compared to the heterologous system [36].

2.4. Functional studies of new $K_V1.3$ inhibitors on T-lymphocytes

To further characterize the effect of the described new $K_V1.3$ inhibitors on T-cell activation, we performed functional studies on PBMC-derived PHA-activated T-lymphocytes. $K_V1.3$ contributes to the maintenance of the electrochemical gradient that controls Ca^{2+} entry into lymphocytes after stimulation by the T-cell receptor, and selective inhibition of $K_V1.3$ is known to be responsible for the perturbation of calcium fluxes. Considering the role of $K_V1.3$ in maintaining the K^+ gradient responsible for Ca^{2+} entry during lymphocyte activation, we examined how the different inhibitors tested affected intracellular $[Ca^{2+}]_i$ levels. After stimulating T-cells with PHA for 5 days, we examined Ca^{2+} levels in the presence of the 3-thiophene-based compounds *cis*-**17** and *trans*-**18**, which had the greatest effect on PBMC PHA-activated T-lymphocytes (56.8 nM and 26.2 nM, respectively) and $K_V1.3$ inhibition on Ltk^- cells (450 nM and 230 nM, respectively). PBMC were stained with the Fluo-4 Ca^{2+} probe, and the Fluo-4 MFI of the $CD3^+$ population was evaluated by flow cytometry after 2 h of inhibition by the compounds (representative histograms Fig. 4B). Mean Fluo-4 fluorescence from 3 replicates normalized to that of the untreated control (Ctrl) for each individual experiment is reported in Fig. 4A. The new $K_V1.3$ inhibitor *trans*-**18** caused a reduction in $[Ca^{2+}]_i$ at a concentration of 5 μM, resulting in reductions of 27% ($p < 0.05$, paired *t*-test), while the compound *cis*-**17** did not reduce intracellular Ca^{2+} levels (Fig. 4A).

Analysis of intracellular Ca^{2+} variations in T-lymphocytes confirmed that physiological Ca^{2+} levels and intracellular TCR signaling are reduced in the presence of $K_V1.3$ inhibitors. The intracellular TCR-mediated signal transduction pathway is essential for the activation of quiescent T-cells and has therefore proven to be a reliable model system for the discovery and evaluation of new immunosuppressive agents. Thus, selective inhibition of $K_V1.3$ could interfere with T-cell activation by modulating the ionic balances that regulate the concentration of physiological Ca^{2+}. Indeed, upon entry into TCR stimulation, Ca^{2+} triggers calcineurin-mediated dephosphorylation of nuclear factor of activated T-cells (NFAT), thereby regulating important cellular processes responsible for cell cycle progression, selection, and differentiation [1]. In this context, we further investigated the effect of new $K_V1.3$ inhibitors on T-cell activation by examining proliferation and colony formation after 5 days of PHA stimulation and treatment with the

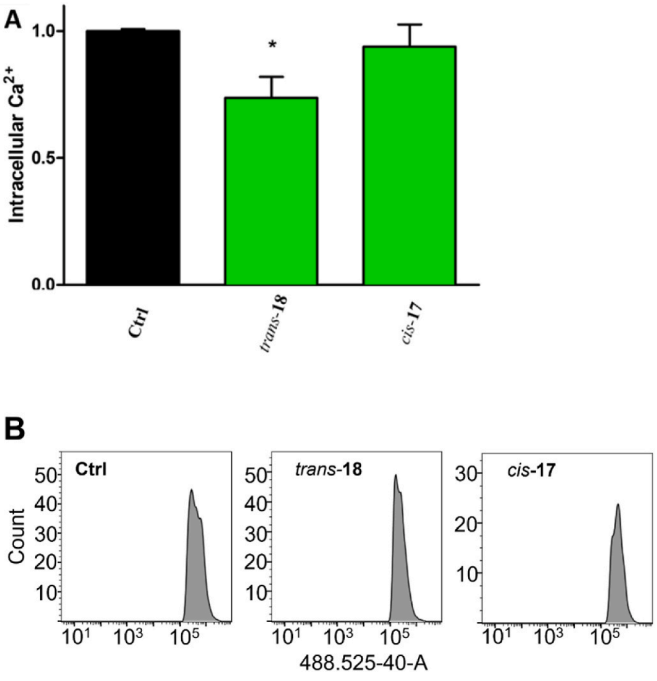

Fig. 4. Effect on intracellular Ca^{2+} levels. Flow cytometry analysis of Fluo-4 fluorescence on $CD3^+$ PBMC. (A) Mean Fluo-4 fluorescence from 3 replicates was normalized to that of the untreated control (Ctrl) for each individual experiment (n = 4). The error bars represent the standard deviation. After activation, cells were treated with the described compounds [5 μM] for 2 h. (B) Representative histograms showing Fluo-4 fluorescence in $CD3^+$ lymphocytes treated with the different compounds and a graph showing a comparison among the different treatment conditions.

compounds.

Because, as mentioned above, Ca^{2+} is one of the most important messengers during lymphocyte activation, the observed reduction in $[Ca^{2+}]_i$ by $K_V1.3$ inhibition suggests that lymphocyte activation may also have changed. To further explore this hypothesis, we investigated how the different compounds affected T-cell activation by examining cell proliferation and T-cell colony formation. Purified PBMC were activated with PHA and cultured at a concentration of 1.5×10^6 cells/mL. Compounds were tested at a concentration of 30 μM to exclude possible inactivation by serum [34]. No effects on viability were noticed and trypan blue staining did not indicate a reduced viability in treated cells compared to untreated (data not shown). We further assessed the proliferation capacity of T cells by counting the cells after 5 days of PHA stimulation and compounds treatment. No effect of the compounds on total cell number emerged (Fig. S9) and after 5 days, the T-cells that formed colonies and the concentration of live cells were counted (Fig. 5, representative colony indicated by the arrow). Image analysis showed a significant decrease in the number of colony-forming units (CFU) after the application of *cis*-**17** and *trans*-**18** (Fig. 5A). The novel compound *trans*-**18** (Fig. 5) showed a correlation with the Ca^{2+} signaling data. This suggests reduced activation of $CD4^+$ T-lymphocytes upon treatment with *trans*-**18**.

To further clarify the mechanism responsible for the observed change in $CD4^+$ colony formation, we examined the effect of the different compounds on cell cycle progression (Fig. 6). On day 5 after PHA activation and treatment, colonies were disaggregated and flow cytometric cell cycle analysis was performed (Fig. 6B). All selected $K_V1.3$ inhibitors showed a significant reduction (Fig. 6A $p < 0.005$) in the fraction of cycling cells (in cell cycle phases S + G2+M), indicating proliferation blockade in phase G0/G1, which could explain the reduced number of colonies observed after treatment.

Compound *trans*-**18**, which inhibited $K_V1.3$ current most potently, impaired intracellular Ca^{2+} signaling and T-cell activation and colony formation. Because $K_V1.3$ has become an important drug target because of its unique role in proliferation and survival of effector memory T-cells [13,14], the selected compounds could be used to modulate channel conductance and thereby alter the processes of lymphoid cell differentiation, selection, proliferation, and migration. Given the critical role of $K_V1.3$ in proliferation [2] and its overexpression in B-cell chronic lymphocytic leukemia (B-CLL) [37], it could confer a survival advantage to proliferating lymphoid cancer cells [13] and provide a target for the treatment of lymphomas and leukemias in which long-term survival rates, particularly in T-cell acute lymphoblastic leukemia (ALL), are still low because of the systemic toxicity of treatments and the occurrence of chemoresistance. In addition, dysregulation of the selective mechanisms could lead to proliferation of lymphocyte clones that are not normally selected, and this could be the basis for expansion of a leukemic clone.

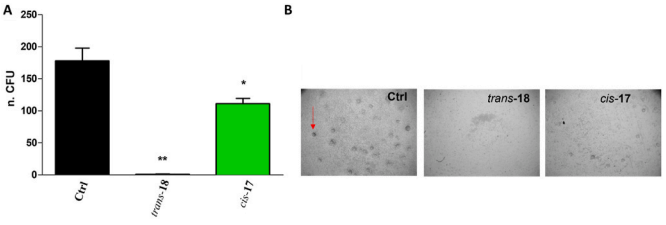

Fig. 5. (A) Bar graph showing the number of T-cell CFUs formed after PHA activation. PBMC were treated with the different drugs [30 μM] together with PHA for 5 days before counting the colonies. Bars represent the mean of 3 experiments, and standard deviation is indicated. (B) Representative images of colonies from A. The arrow shows a representative colony. Images were taken with a bright-field microscope.

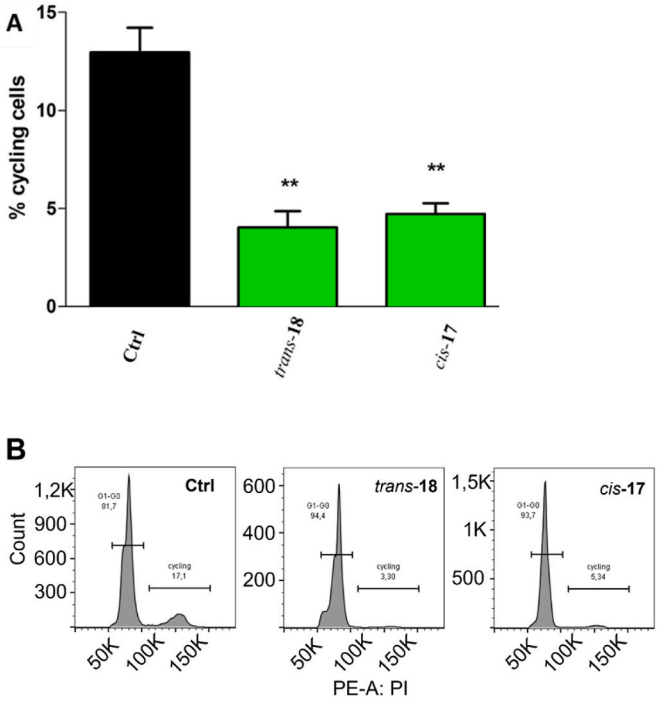

Fig. 6. Flow cytometry cell cycle analysis of PBMC after 5 days of PHA stimulation and treatment with the described drugs [30 μM]. (A) Bars represent the mean of the percentage of cycling cells (S + G2+M) from 3 experiments. Error bars represent the standard deviation between replicates. Unpaired *t*-test was performed to compare drug-treated and untreated (Ctrl) samples (*: $p < 0.05$; **: $p < 0.005$. (B) Representative histograms showing activated T-lymphocytes at different stages of cell cycle progression, grouped in G0/G1 and in cycling (cell cycle phases S + G2+M) as shown in A.

3. Conclusion

New thiophene-based $K_V1.3$ inhibitors were discovered by structural optimization of previously published compound **6**. The new optimized $K_V1.3$ inhibitors exhibited 2- to 6-fold higher $K_V1.3$ inhibition on Ltk^- cells than compound **6** in the nanomolar range. The new 3-thiophene-based propyl carbamate analog (*trans*-**18**) and the alcohol analog (*cis*-**17**) inhibited $K_V1.3$ channels in the nanomolar range in three independent test systems on *Xenopus laevis* oocytes, Ltk^- cells, and PHA-activated T-lymphocytes. Functional studies on PHA-activated T-lymphocytes from PBMC showed that inhibitor *trans*-**18**, the most potent $K_V1.3$ inhibitors on T-lymphocytes, impaired intracellular Ca^{2+} signaling and T-cell activation, proliferation, and colony formation. Taken together, these results suggest that these newly synthesized $K_V1.3$ inhibitors may represent basis for further optimization, but more detailed studies based on cellular disease models are needed.

4. Experimental section

4.1. Materials

The reagents and solvents used were obtained from commercial sources (i.e., Acros Organics, Sigma-Aldrich, TCI Europe, Merck, Carlo Erba, Apollo Scientific) and were used as provided. Anhydrous THF was prepared by distillation over sodium and benzophenone under $Ar_{(g)}$. Analytical thin-layer chromatography was performed on silica gel aluminum sheets (60 F254, 0.20 mm; Merck). Flash column chromatography was performed on silica gel 60 (particle size 0.040–0.063 mm, Merck). Reversed-phase column chromatography (RP-CC) was performed on the Isolera Biotage One Flash Chromatography system (SNAP Biotage KP-C18-HS column, 12 g, Biotage, Uppsala, Sweden) using a

gradient of 0.1% TFA in deionised water and MeCN as eluent (gradient 10–100% MeCN in 15 column volumes (300 mL); 100% MeCN for 5 column volumes (100 mL)). ^{1}H NMR and ^{13}C spectra were recorded at 400 and 100 MHz, respectively, on a Bruker Avance III NMR spectrometer (Bruker, MA, USA) at 295 K. The chemical shifts (δ) are reported in ppm and are referenced to the deuterated solvent used. HRMS measurements were performed on a LC–MS/MS system (Q Executive Plus; Thermo Scientific, MA, USA). Mass spectrometry measurements were performed on an Expression CMS^{L} mass spectrometer (Advion, NY, USA). Analytical reversed-phase UPLC analyses were performed using a modular system (Thermo Scientific Dionex UltiMate 3000 modular system; Thermo Fisher Scientific Inc., MA, USA). Method: Waters Acquity UPLC® HSS C18 SB column (2.1 × 50 mm, 1.8 μm), T = 40 °C; injection volume = 5 μL; flow rate = 0.4 mL/min; detector λ = 254 nm; mobile phase A (0.1% trifluoroacetic acid (TFA) [v/v] in water), mobile phase B acetonitrile (MeCN). Gradient: 0–2 min, 10% B; 2–10 min, 10%–90% B; 10–12 min, 90% B. Purities of the tested compounds were established to be ≥ 95% at 254 nm, as determined by UPLC.

Compounds **3**, *trans*-**4**, and *cis*-**4** were resynthesized according to Scheme S1 as previously reported [27]. Analytical data for compounds **3**, *trans*-**4**, and *cis*-**4**, and their precursors is given in the Supporting Information. Compound **6** was prepared as previously described by our group [27]. The analytical data here were identical to those reported previously.

4.2. General synthetic chemistry experimental protocols

4.2.1. General procedure A: synthesis of diester intermediates

Corresponding thiophene acetonitrile (75 mmol, 1.0 equiv) and methyl acrylate (375 mmol, 5.0 equiv) were dissolved in *tert*-butanol (45 mL) at room temperature and heated to boiling point. The heating source was then removed and benzyltrimethylammonium hydroxide (75 mmol, 1.0 equiv), dissolved in *tert*-butanol (10 mL), was added dropwise at room temperature. The reaction mixture was stirred under reflux for 4 h and then cooled to room temperature overnight. Next day toluene (100 mL) and water (70 mL) were added to reaction mixture. The organic phase was separated and washed with water (2 × 70 mL), saturated brine solution (50 mL), dried over Na_2SO_4, filtered, and the solvent evaporated under reduced pressure. The product was used without further purification.

4.2.2. General procedure B: synthesis of 4-aryl-4-cyano-2-carbomethoxy-cyclohexanone derivatives

Appropriate cyanothiopheneheptanedioate (61 mmol, 1.0 equiv) was dissolved in anhydrous THF (250 mL) under argon atmosphere. Potassium *tert*-butoxide (122 mmol, 2 equiv) was added in portions with cooling on ice. The reaction mixture was stirred under reflux for 5 h and cooled to room temperature overnight. Next day 2.5 M acetic acid (220 mL) was added dropwise with cooling on ice. The batch was mixed with toluene (150 mL). Organic phase was separated and washed with saturated aqueous $NaHCO_3$ solution (3 × 100 mL), water (3 × 100 mL) and saturated brine solution (75 mL). After drying over Na_2SO_4, the solvent was evaporated. The product was used without further purification unless stated otherwise.

4.2.3. General procedure C: synthesis of 4,4-disubstituted cyclohexanones

Corresponding methyl 2-oxocyclohexane-1-carboxylate (47 mmol, 1.0 equiv) was dissolved in 10% sulfuric acid (170 mL) and glacial acetic acid (380 mL). The reaction mixture was boiled at 100 °C for 24 h. The batch was then cooled to room temperature and diluted with water (500 mL) on ice bath. The water phase was extracted with ethyl acetate (3 × 150 mL) and combined organic phases were thoroughly washed with saturated aqueous $NaHCO_3$ solution (5 × 100 mL), water (5 × 100 mL), saturated brine solution (100 mL), dried over Na_2SO_4, filtered and evaporated. When ethyl acetate (25 mL) was added to crude product, white precipitate was formed. White precipitate was removed by filtration and dried. The product was additionally purified by flash column chromatography.

4.2.4. General procedure D: introduction of protection group to ketone derivatives

Ketone derivative (29 mmol, 1.0 equiv) was dissolved in toluene (300 mL). Ethane-1,2-diol (290 mmol, 10.0 equiv) and PTSA (0.58 mmol, 0.02 equiv.) were added to reaction mixture. The flask was boiled at 140 °C in Dean-Stark apparatus overnight. Next day the flask was cooled to room temperature and the solvent was evaporated. Product was dissolved in ethyl acetate (400 mL) and washed with saturated aqueous $NaHCO_3$ solution (2 × 150 mL), water (2 × 150 mL) and saturated brine solution (150 mL). Organic phase was dried over Na_2SO_4, filtered and evaporated under reduced pressure. The product was additionally purified by flash column chromatography.

4.2.5. General procedure E: reduction of carbonitrile to amine derivatives

Carbonitrile intermediate (27 mmol, 1.0 equiv.) was dissolved in anhydrous THF (100 mL) under argon atmosphere with cooling on ice. $LiAlH_4$ (54 mmol, 2.0 equiv.) was added in portions on ice bath and batch was stirred at room temperature overnight. For workup, diethylether (300 mL) was added to flask with cooling on ice and then saturated brine solution (5–10 mL) was slowly added while the batch was stirred on ice bath. Residual water was removed by addition of Na_2SO_4. Precipitate was filtered off and additionally washed with diethylether. Organic solvent was removed under reduced pressure and the product was used without further purification unless stated otherwise.

4.2.6. General procedure F: synthesis of benzamide analogs

Benzoic acid derivative (26 mmol, 1.0 equiv) was dissolved in DCM (100 mL) with cooling on ice. Oxalyl chloride (78 mmol, 3.0 equiv) was added dropwise, followed by 5 drops of DMF. The batch was stirred at room temperature overnight and next day the solvent was evaporated. Appropriate amine (26 mmol, 1.0 equiv) and Et_3N (78 mmol, 3.0 equiv.) were dissolved in DCM (75 mL) with cooling on ice, followed by addition of benzoyl chloride intermediate (26 mmol, 1.0 equiv), dissolved in DCM (75 mL). Reaction mixture was stirred at room temperature overnight. Organic phase was then diluted with 75 mL of DCM and washed with saturated aqueous $NaHCO_3$ solution (2 × 50 mL), 1 M aqueous HCl solution, water (2 × 50 mL), saturated brine solution (50 mL), dried over Na_2SO_4, filtered and remained organic phase was removed under reduced pressure. The product was used without further purification unless stated otherwise.

4.2.7. General procedure G: removal of protection group from ketone

Benzamide analog (23 mmol, 1.0 equiv) was dissolved in acetone (150 mL), followed by the addition of pyridinium *p*-toluenesulfonate (2.3 mmol, 0.1 equiv) and water (20 mL). The reaction mixture was stirred at reflux for 48 h, and then the solvent was evaporated. The residue was dissolved in DCM (200 mL) and washed with aqueous $NaHCO_3$ solution (50 mL), 1 M aqueous HCl solution (50 mL), water (2 × 50 mL), and saturated brine solution (50 mL). Organic phase was dried over Na_2SO_4, filtered and the solvent removed under reduced pressure. The product was purified by flash column chromatography.

4.2.8. General procedure H: reduction of ketone group to hydroxyl group

Benzamide derivative (17 mmol, 1.0 equiv) was dissolved in anhydrous THF (100 mL) under argon atmosphere with cooling on ice. $NaBH_4$ (34 mmol, 2.0 equiv) was then added in portions with cooling on ice and the batch was stirred at room temperature overnight. Next day, 1 M aqueous HCl solution (100 mL) was added to reaction mixture with cooling on ice and extracted with DCM (2 × 100 mL). Combined organic phases were then washed with water (50 mL), dried over Na_2SO_4, filtered and the solvent removed under reduced pressure. Product was purified by flash column chromatography. *Trans* (5.8 mmol) and *cis* (9.7

mmol) derivatives were separated by flash column chromatography.

4.2.9. General procedure I: synthesis of carbamate derivatives from alcohols

Hydroxyl analog (0.6 mmol or 1.2 mmol, 1.0 equiv.) was dissolved in DCM (50 mL) and then Et_3N (3 mmol or 6 mmol, 5.0 equiv) was slowly added. The flask was stirred at room temperature for 5 min and then 4-nitrophenyl chloroformate (1.2 mmol or 2.4 mmol, 2.0 equiv.) was added in portions. Reaction mixture was stirred at room temperature overnight and then washed with water (25 mL), 1 M aqueous HCl solution (25 mL), and saturated brine solution (25 mL). Organic phase was dried over Na_2SO_4, filtered and the solvent removed under reduced pressure. Intermediate (0.3 mmol or 0.6 mmol, 1.0 equiv.) was dissolved in DCM (50 mL) and then amine (3 mmol or 6 mmol, 10.0 equiv.) was added at room temperature. The flask was stirred at room temperature overnight and next day washed with water (25 mL), 1 M aqueous HCl solution (25 mL), and saturated brine solution (25 mL). Organic phase was dried over Na_2SO_4, filtered, and the solvent removed under reduced pressure. Product was additionally purified by flash column chromatography.

4.2.10. General procedure J: synthesis of azide derivatives

Corresponding hydroxyl analog (2 mmol, 1.0 equiv.) was dissolved in DCM (25 mL) with cooling on ice followed by addition of Et_3N (4 mmol, 2.0 equiv). Methanesulfonyl chloride (4 mmol, 2 equiv) was added dropwise and the flask was stirred with cooling on ice for 2 h. Reaction mixture was washed with water (3 × 10 mL) and solvent was removed under reduced pressure. Intermediate (2 mmol, 1.0 equiv.) was dissolved in anhydrous DMF (30 mL) followed by addition of sodium azide (4 mmol, 2.0 equiv.). The flask was stirred at 100 °C overnight. Next day, the solvent was removed under reduced pressure and product was purified by flash column chromatography.

4.2.11. General procedure K: reduction of azide to amine derivatives

Azide intermediate (1.1 mmol, 1.0 equiv.) was dissolved in ethyl acetate (50 mL) and purged under a stream of argon for 10 min. Catalytic amount of Pd/C (10% load on carbon, 10–20% [w/w] calculated to the starting material) was added, and the resulting suspension mixture was stirred under H_2 (g) atmosphere at room temperature for 16–24 h. The catalyst was removed by filtration through Celite and evaporated to obtain crude product. The amine intermediate (1 mmol) was used without further purification unless stated otherwise.

4.2.12. General procedure L: formation of amine salts with HCl

Amine intermediate (0.3 mmol, 1 equiv.) was dissolved in MeOH and then 4 M HCl solution (3 mmol, 10 equiv) in 1,4-dioxane was added dropwise. The flask was stirred at room temperature for 1 h and the solvent was removed under reduced pressure. Product was purified by reversed-phase chromatography (Biotage SNAP Cartridge KP-C18-HS 12 g column), MF: gradient water in H_2O/acetonitrile.

4.3. Synthesis and characterization of intermediates and inhibitors

4.3.1. 2-Methoxy-5-methyl-N-((4-oxo-1-(thiophen-2-yl)cyclohexyl)methyl)benzamide (7)

Synthesized from **30** (507 mg, 2.0 mmol, 1.0 equiv), Et_3N (0.84 mL, 6.0 mmol, 3.0 equiv) and 2-methoxy-5-methylbenzoyl chloride (369 mg, 2.0 mmol, 1.0 equiv) via general procedure F and pyridinium *p*-toluenesulfonate (45 mg, 0.18 mmol, 0.1 equiv) and water (8 mL) via general procedure G. Column chromatography, EtOAc/*n*-hexane = 1/2 (v/v). Yield: 40% (289 mg); white solid. ^{1}H NMR (400 MHz, DMSO-d_6): δ 2.06–2.17 (2H, m, H_a-2,6), 2.26 (3H, s, H-20′, H-20′′, H-20‴), 2.26–2.42 (6H, m, H_a-3,5, H_e-3,5, H_e-2,6), 3.63 (2H, d, J = 6.1 Hz, H-7′, H-7′′), 3.72 (3H, s, OC$\underline{H}_3$), 7.01 (1H, d, J = 8.5 Hz, H-11), 7.11 (1H, dd, J_1 = 5.0 Hz, J_2 = 3.5 Hz, H-18), 7.16 (dd, J_1 = 3.5 Hz, J_2 = 1.1 Hz, H-17), 7.27 (1H, dd, J_1 = 8.4 Hz, J_2 = 1.9 Hz, H-12), 7.54 (1H, dd, J_1 = 5.1 Hz, J_2 = 1.1 Hz, H-19), 7.63 (1H, d, J = 2.1 Hz, H-14), 7.96 (1H, t, J = 5.9 Hz, N$\underline{H}$CO). ^{13}C NMR (101 MHz, DMSO-d_6) δ 19.92 (C-20), 34.14 (C-2,6), 37.20 (C-3,5), 41.50 (C-1), 49.64 (C-7), 55.87 (C-15), 112.10 (C-11), 121.42 (C-9), 124.87 (C-19), 125.05 (C-17), 127.22 (C-18), 129.45 (C-13), 131.06 (C-14), 132.85 (C-12), 148.37 (C-16), 155.04 (C-10), 164.71 (C-8), 209.72 (C-4). HRMS (ESI+): *m/z* calcd for $[M + H]^+$ 358.1471; found 358.1470. HPLC purity, 99.9% at 254 nm (t_R = 4.96 min).

4.3.2. 5-Fluoro-2-methoxy-N-((4-oxo-1-(thiophen-2-yl)cyclohexyl)methyl)benzamide (8)

Synthesized from **30** (1.27 g, 5.0 mmol, 1.0 equiv), Et_3N (2.09 mL, 15.0 mmol, 3.0 equiv) and 5-fluoro-2-methoxybenzoyl chloride (943 mg, 5.0 mmol, 1.0 equiv) via general procedure F, and pyridinium *p*-toluenesulfonate (121 mg, 0.48 mmol, 0.1 equiv) and water (10 mL) via general procedure G. Column chromatography, EtOAc/*n*-hexane = 1/2 (v/v). Yield: 50% (901 mg); white solid. ^{1}H NMR (400 MHz, DMSO-d_6): δ 2.06–2.18 (2H, m, H_a-2,6), 2.25–2.42 (6H, m, H_e-2,6, H_a-3,5, H_e-3,5), 3.62 (2H, d, J = 6.1 Hz, H-7′, H-7′′), 3.76 (3H, s, OC$\underline{H}_3$), 7.11 (1H, dd, J_1=5.1 Hz, J_2=3.5 Hz, H-18), 7.13–7.19 (2H, m, H-11, H-17), 7.33 (1H, ddd, J_1=9.0 Hz, J_2 = 7.8 Hz, J_3 = 3.4 Hz, H-12), 7.52 (1H, dd, J_1=9.5 Hz, J_2=3.5 Hz, H-14), 7.55 (1H, dd, J_1=5.2 Hz, J_2 = 1.1 Hz, H-19), 8.05 (1H, t, J = 6.0 Hz, N$\underline{H}$CO). ^{13}C NMR (101 MHz, DMSO-d_6) δ 34.11 (C-2,6), 37.18 (C-3,5), 41.53 (C-1), 49.83 (C-7), 56.47 (C-15), 113.97 (d, J = 7.8 Hz, C-11), 116.56 (d, J = 24.7 Hz, C-14), 118.71 (d, J = 23.0 Hz, C-12), 123.48 (d, J = 6.6 Hz, C-9), 124.91 (C-19), 125.16 (C-17), 127.24 (C-18), 148.16 (C-16), 153.36 (d, J = 1.7 Hz, C-10), 156.04 (d, J = 237.0 Hz, C-13), 163.57 (d, J = 1.7 Hz, C-8), 209.67 (C-4). HRMS (ESI+): *m/z* calcd for $[M + H]^+$ 362.1221; found 362.1216. HPLC purity, 99.1% at 254 nm (t_R = 4.74 min).

4.3.3. N-((4-oxo-1-(thiophen-2-yl)cyclohexyl)methyl)furan-3-carboxamide (9)

Synthesized from **30** (1.27 g, 5.0 mmol, 1.0 equiv), Et_3N (2.09 mL, 15.0 mmol, 3.0 equiv) and furan-3-carbonyl chloride (653 mg, 5.0 mmol, 1.0 equiv) via general procedure F, and pyridinium *p*-toluenesulfonate (100 mg, 0.40 mmol, 0.1 equiv) and water (10 mL) via general procedure G. Column chromatography, EtOAc/*n*-hexane = 1/2 (v/v). Yield: 52% (794 mg); white solid. ^{1}H NMR (400 MHz, DMSO-d_6): δ 2.03–2.17 (2H, m, H_a-2,6), 2.23–2.34 (6H, m, H_a-3,5, H_e-3,5, H_e-2,6), 3.42 (2H, d, J = 6.5 Hz, H-7′, H-7′′), 6.83 (1H, dd, J_1=1.9 Hz, J_2=0.8 Hz, H-12), 7.04 (1H, dd, J_1=5.1 Hz, J_2=3.5 Hz, H-15), 7.10 (1H, dd, J_1=3.5 Hz, J_2=1.1 Hz, H-14), 7.47 (1H, dd, J_1=5.1 Hz, J_2=1.1 Hz, H-16), 7.70 (1H, t, J = 1.7 Hz, H-11), 8.05 (1H, brt, J = 6.4 Hz, N$\underline{H}$CO), 8.18 (1H, dd, J_1=1.5 Hz, J_2=0.8 Hz, H-10). ^{13}C NMR (101 MHz, DMSO-d_6) δ 34.03 (C-2,6), 37.27 (C-3,5), 42.27 (C-1), 49.63 (C-7), 109.16 (C-12), 122.63 (C-9), 124.65 (C-16), 124.89 (C-14), 127.13 (C-15), 143.84 (C-11), 145.15 (C-10), 147.84 (C-13), 161.96 (C-8), 209.78 (C-4). HRMS (ESI+): *m/z* calcd for $[M + H]^+$ 304.1002; found 304.1000. HPLC purity, 99.6% at 254 nm (t_R = 3.40 min).

4.3.4. 2-Methoxy-4-methyl-N-((4-oxo-1-(thiophen-2-yl)cyclohexyl)methyl)benzamide (10)

Synthesized from **30** (507 mg, 2.0 mmol, 1.0 equiv), Et_3N (0.84 mL, 6.0 mmol, 3.0 equiv) and 2-methoxy-4-methylbenzoyl chloride (369 mg, 2.0 mmol, 1.0 equiv) via general procedure F, and pyridinium *p*-toluenesulfonate (28 mg, 0.11 mmol, 0.1 equiv) and water (8 mL) via general procedure G. Column chromatography, EtOAc/*n*-hexane = 1/2 (v/v). Yield: 29% (201 mg); white solid. ^{1}H NMR (400 MHz, DMSO-d_6): δ 2.05–2.16 (2H, m, H_a-2,6), 2.24–2.42 (6H, m, H_a-3,5, H_e-3,5, H_e-2,6), 2.33 (3H, s, H-20′, H-20′′, H-20‴), 3.63 (2H, d, J = 6.1 Hz, H-7′, H-7′′), 3.75 (3H, s, OC$\underline{H}_3$), 6.81–6.89 (1H, m, H-13), 6.95 (1H, s, H-11), 7.12 (1H, dd, J_1=5.1 Hz, J_2 = 3.5 Hz, H-18), 7.16 (1H, dd, J_1=3.5 Hz, J_2 = 1.2 Hz, H-17), 7.55 (1H, dd, J_1=5.1 Hz, J_2 = 1.2 Hz, H-19), 7.75 (1H, d, J = 7.9 Hz, H-14), 7.89 (1H, t, J = 6.0 Hz, CON$\underline{H}$). ^{13}C NMR (101 MHz, DMSO-d_6) δ 21.19 (C-20), 34.16 (C-2,6), 37.18 (C-3,5), 41.45 (C-1),

49.61 (C-7), 55.76 (C-15), 112.64 (C-11), 118.80 (C-9), 121.40 (C-13), 124.88 (C-19), 125.04 (C-17), 127.23 (C-18), 130.94 (C-14), 143.04 (C-12), 148.39 (C-16), 157.05 (C-10), 164.51 (C-8), 209.69 (C-4). HRMS (ESI+): *m/z* calcd for $[M + H]^+$ 358.1471; found 358.1467. HPLC purity, 99.7% at 254 nm (t_R = 4.91 min).

4.3.5. *N-(((1S,4S)-4-Hydroxy-1-(thiophen-2-yl)cyclohexyl)methyl)-2-methoxybenzamide (cis-11)*

Synthesized from **14** (5.50 g, 15.9 mmol, 1.0 equiv) and $NaBH_4$ (1.20 g, 31.8 mmol, 2.0 equiv) via general procedure H. Column chromatography, DCM/diethyl ether = 2/1 (v/v). Yield: 31% (1.7 g); white solid. ^{1}H NMR (400 MHz, DMSO-d_6): δ_H 1.20–1.32 (2H, m, H_a-3,5), 1.57–1.67 (2H, m, H_a-2,6), 1.68–1.75 (2H, m, H_e-3,5), 2.05–2.13 (2H, m, H_e-2,6), 3.41 (2H, d, J = 6.0 Hz, H-7′, H-7′′), 3.41–3.51 (1H, m, H-4), 3.78 (3H, s, OC$\underline{H}_3$), 4.45 (1H, d, J = 4.6 Hz, O$\underline{H}$), 7.01 (1H, dd, J_1 = 3.4 Hz, J_2 = 1.2 Hz, H-17), 7.01–7.05 (1H, m, H-13), 7.08 (1H, dd, J_1 = 5.1 Hz, J_2 = 3.5 Hz, H-18), 7.12 (1H, dd, J_1 = 8.4 Hz, J_2 = 1.0 Hz, H-11), 7.43–7.47 (1H, m, H-12), 7.48 (1H, dd, J_1 = 5.1 Hz, J_2 = 1.1 Hz, H-19), 7.82 (1H, dd, J_1 = 7.7 Hz, J_2 = 1.8 Hz, H-14), 7.85 (1H, brt, J = 6.0 Hz, N$\underline{H}$CO). ^{13}C NMR (101 MHz, DMSO-d_6): δ_C 30.95 (C-3,5), 32.58 (C-2,6), 41.74 (C-1), 51.71 (C-7), 55.86 (C-15), 68.10 (C-4), 112.11 (C-11), 120.65 (C-13), 121.87 (C-9), 124.42 (C-19), 124.61 (C-17), 127.09 (C-18), 130.83 (C-14), 132.52 (C-12), 149.72 (C-16), 157.04 (C-10), 164.44 (C-8). HRMS (ESI+): *m/z* calcd for $[M + H]^+$ 346.1471; found 346.1457. HPLC purity, 96.6% at 254 nm (t_R = 4.00 min).

4.3.6. *N-(((1R,4R)-4-Hydroxy-1-(thiophen-2-yl)cyclohexyl)methyl)-2-methoxybenzamide (trans-11)*

Synthesized from **14** (5.50 g, 15.9 mmol, 1.0 equiv) and $NaBH_4$ (1.20 g, 31.8 mmol, 2.0 equiv) via general procedure H. Column chromatography, DCM/diethyl ether = 2/1 (v/v). Yield: 43% (2.4 g); white solid. ^{1}H NMR (400 MHz, DMSO-d_6): δ_H 1.50–1.65 (4H, m, H_e-3,5, H_a-3,5), 1.67–1.76 (2H, m, H_a-2,6), 1.93–2.03 (2H, m, H_e-2,6), 3.51–3.61 (3H, m, H-4, H-7′, H-7′′), 3.73 (3H, s, OC$\underline{H}_3$), 4.53 (1H, d, J = 3.7 Hz, O$\underline{H}$), 6.99–7.09 (3H, m, H-17, H-13, H-18), 7.11 (1H, d, J = 8.3 Hz, H-11), 7.44–7.49 (2H, m, H-12, H-19), 7.81 (1H, brt, J = 5.9 Hz, N$\underline{H}$CO), 7.89 (1H, d, J = 7.8 Hz, H-14). ^{13}C NMR (101 MHz, DMSO-d_6): δ_C 30.00 (C-3,5), 31.28 (C-2,6), 41.04 (C-1), 48.56 (C-7), 55.80 (C-15), 66.09 (C-4), 112.15 (C-11), 120.71 (C-13), 121.38 (C-9), 123.92 (C-19), 124.08 (C-17), 126.87 (C-18), 131.02 (C-14), 132.68 (C-12), 151.28 (C-16), 157.12 (C-10), 164.20 (C-8). HRMS (ESI+): *m/z* calcd for $[M + H]^+$ 346.1471; found 346.1457. HPLC purity, 96.1% at 254 nm (t_R = 4.36 min).

4.3.7. *(1S,4S)-4-((2-Methoxybenzamido)methyl)-4-(thiophen-2-yl) cyclohexyl methylcarbamate (cis-12)*

Synthesized from *cis*-**11** (215 mg, 0.6 mmol, 1 equiv), 4-nitrophenyl chloroformate (242 mg, 1.2 mmol, 2 equiv), Et_3N (0.25 mL, 1.8 mmol, 3 equiv) and methyl amine (186 mg, 6 mmol, 10 equiv) via general procedure I. Column chromatography, EtOAc/*n*-hexane = 1/1 (v/v). Two conformers in a 1:9 ratio. Yield: 48% (120 mg); white solid. ^{1}H NMR (400 MHz, DMSO-d_6) for both conformers: δ_H 1.33–1.48 (2H, m, H_a-3,5), 1.67–1.79 (2H, m, H_a-2,6), 1.79–1.89 (2H, m, H_e-3,5), 2.06–2.14 (2H, m, H_e-2,6), 2.52 (3H, d, J = 4.5 Hz, CONHC$\underline{H}_3$), 3.45 (2H, d, J = 6.0 Hz, H-7′, H-7′′), 3.78 (3H, s, OC$\underline{H}_3$), 4.50–4.60 (1H, m, H-4), 6.83 (1H, q, J = 4.5 Hz, CON$\underline{H}$CH$_3$), 7.00–7.03 (1H, m, H-13), 7.04 (1H, dd, J_1 = 3.2 Hz, J_2 = 1.1 Hz, H-17), 7.08 (1H, dd, J_1 = 5.2 Hz, J_2 = 3.2 Hz, H-18), 7.12 (1H, dd, J_1 = 8.4 Hz, J_2 = 0.9 Hz, H-11), 7.47 (1H, ddd, J_1 = 8.4 Hz, J_2 = 7.3 Hz, J_3 = 1.9 Hz, H-12), 7.49 (1H, dd, J_1 = 5.2 Hz, J_2 = 1.1 Hz, H-19), 7.80 (1H, dd, J_1 = 7.7 Hz, J_2 = 1.9 Hz, H-14), 7.89 (1H, brt, J = 6.0 Hz, CH$_2$N$\underline{H}$CO). ^{13}C NMR (101 MHz, DMSO-d_6) for both conformers: δ_C 26.81 (C-21), 27.43 (C-3,5), 32.02 (C-2,6), 41.60 (C-1), 50.96 (C-7), 55.83 (C-15), 71.04 (C-4), 112.09 (C-11), 120.64 (C-13), 122.02 (C-9), 124.53 (C-19), 124.67 (C-17), 127.11 (C-18), 130.75 (C-14), 132.48 (C-12), 149.41 (C-16), 156.22 (C-20), 157.00 (C-10), 164.57 (C-8). HRMS (ESI+): *m/z* calcd for $[M + H]^+$ 403.1686; found 403.1681. HPLC purity, 100.0% at 254 nm (t_R = 4.77 min).

4.3.8. *(1R,4R)-4-((2-Methoxybenzamido)methyl)-4-(thiophen-2-yl) cyclohexyl methylcarbamate (trans-12)*

Synthesized from *trans*-**11** (215 mg, 0.6 mmol, 1 equiv), 4-nitrophenyl chloroformate (242 mg, 1.2 mmol, 2 equiv), Et_3N (0.25 mL, 1.8 mmol, 3 equiv) and methyl amine (186 mg, 6 mmol, 10 equiv) via general procedure I. Column chromatography, EtOAc/*n*-hexane = 1/1 (v/v). Two conformers in a 12:88 ratio. Yield: 44% (110 mg); white solid. ^{1}H NMR (400 MHz, DMSO-d_6) for both conformers: δ_H 1.62–1.74 (4H, m, H_e-3,5, H_a-3,5), 1.78–2.09 (4H, m, H_e-2,6, H_a-2,6), 2.56 (3H, d, J = 4.6 Hz, NHC$\underline{H}_3$), 3.58 (2H, d, J = 5.9 Hz, H-7′, H-7′′), 3.72 (3H, s, OC$\underline{H}_3$), 4.56–4.63 (1H, m, H-4), 6.98 (1H, q, J = 4.5 Hz, CON$\underline{H}$CH$_3$), 7.01–7.06 (2H, m, H-13, H-17), 7.08 (1H, dd, J_1 = 5.1 Hz, J_2 = 3.5 Hz, H-18), 7.11 (1H, dd, J_1 = 8.4, J_2 = 1.0 Hz, H-11), 7.47 (1H, ddd, J_1 = 8.4 Hz, J_2 = 7.3 Hz, J_3 = 1.9 Hz, H-12), 7.49 (1H, dd, J_1 = 5.1 Hz, J_2 = 1.1 Hz, H-19), 7.80 (1H, brt, J = 5.9 Hz, CH$_2$N$\underline{H}$CO), 7.88 (1H, dd, J_1 = 7.7 Hz, J_2 = 1.9 Hz, H-14). ^{13}C NMR (101 MHz, DMSO-d_6) for both conformers: δ_C 26.76 (C-21), 26.85 (C-3,5), 31.06 (C-2,6), 41.06 (C-1), 49.13 (C-7), 55.81 (C-15), 69.45 (C-4), 112.16 (C-11), 120.70 (C-13), 121.30 (C-9), 124.29 (C-19), 124.34 (C-17), 126.99 (C-18), 131.01 (C-14), 132.71 (C-12), 150.19 (C-16), 156.28 (C-20), 157.12 (C-10), 164.27 (C-8). HRMS (ESI+): *m/z* calcd for $[M + H]^+$ 403.1686; found 403.1682. HPLC purity, 98.0% at 254 nm (t_R = 4.85 min).

4.3.9. *(1R,4R)-4-((2-Methoxybenzamido)methyl)-4-(thiophen-2-yl) cyclohexyl (3-methoxypropyl)carbamate (trans-13)*

Synthesized from *trans*-**11** (103 mg, 0.3 mmol, 1.0 equiv), 4-nitrophenyl chloroformate (121 mg, 0.6 mmol, 2.0 equiv), Et_3N (0.13 mL, 0.90 mmol, 3.0 equiv) and 3-methoxypropylamine (0.31 mL, 3.0 mmol, 10.0 equiv) via general procedure I. Column chromatography, EtOAc/*n*-hexane = 1/1 (v/v). Two conformers in a 11:89 ratio. Yield: 49% (68 mg); white solid. ^{1}H NMR (400 MHz, DMSO-d_6) for both conformers: 1.57–1.65 (2H, m, H-22′, H-22′′), 1.65–1.77 (4H, m, H_e-3,5, H_a-3,5), 1.79–1.99 (4H, m, H_e-2,6, H_a-2,6), 3.02 (2H, dd, J_1=13.0 Hz, J_2 = 6.7 Hz, H-21′, H-21′′), 3.21 (3H, s, H-24′, H-24′′, H-24‴), 3.32 (2H, t, J = 6.3 Hz, H-23′, H-23′′), 3.59 (2H, d, J = 5.6 Hz, H-7′, H-7′′), 3.73 (3H, s, OC$\underline{H}_3$), 4.59 (1H, brs, H-4), 7.01–7.15 (5H, m, OCON$\underline{H}$CH$_2$, H-11, H-13, H-17, H-18), 7.42–7.54 (2H, m, H-12, H-19), 7.81 (1H, t, J = 5.6 Hz, CH$_2$N$\underline{H}$CO), 7.89 (1H, dd, J_1 = 7.7 Hz, J_2 = 1.7 Hz, H-14). ^{13}C NMR (101 MHz, $CDCl_3$) for both conformers: δ 26.77 (C-3,5), 29.56 (C-22), 31.09 (C-2,6), 37.43 (C-21), 41.06 (C-1), 49.12 (C-7), 55.82 (C-15), 57.89 (C-24), 69.45 (C-4), 69.52 (C-23), 112.18 (C-11), 120.72 (C-13), 121.31 (C-9), 124.30 (C-19), 124.36 (C-17), 127.00 (C-18), 131.04 (C-14), 132.73 (C-12), 150.25 (C-16), 155.78 (C-20), 157.15 (C-10), 164.30 (C-8). HRMS (ESI+): *m/z* calcd for $[M + H]^+$ 461.2105; found 461.2104. HPLC purity, 100% at 254 nm (t_R = 5.14 min).

4.3.10. *2-Methoxy-N-((4-oxo-1-(thiophen-2-yl)cyclohexyl)methyl) benzamide (14)*

Synthesized from **32** (8.40 g, 21.7 mmol, 1.0 equiv), pyridinium *p*-toluenesulfonate (0.55 g, 2.2 mmol, 0.1 equiv) and water (20 mL) via general procedure G. Column chromatography, EtOAc/*n*-hexane = 1/1 (v/v). Yield: 75% (5.50 g); white solid. ^{1}H NMR (400 MHz, $CDCl_3$): δ 2.12–2.24 (2H, m, H_a-2,6), 2.37–2.53 (6H, m, H_a-3,5, H_e-2,6, H_e-3,5), 3.75 (3H, s, OC$\underline{H}_3$), 3.80 (2H, d, J = 6.2 Hz, H-7′, H-7′′), 6.92 (1H, d, J = 8.3 Hz, H-11), 7.03–7.08 (2H, m, H-17, H-13), 7.09 (1H, dd, J_1 = 5.1 Hz, J_2 = 3.6 Hz, H-18), 7.35 (1H, dd, J_1 = 5.1 Hz, J_2 = 1.1 Hz, H-19), 7.43 (1H, ddd, J_1 = 8.4 Hz, J_2 = 7.3 Hz, J_3 = 1.9 Hz, H-12), 7.88 (1H, t, J = 5.3 Hz, N$\underline{H}$CO), 8.20 (1H, dd, J_1 = 7.8 Hz, J_2 = 1.8 Hz, H-14). ^{13}C NMR (100 MHz, $CDCl_3$): δ 35.09 (C-2,6), 37.70 (C-3,5), 42.09 (C-1), 50.70 (C-7), 55.65 (C-15), 111.27 (C-11), 121.03 (C-9), 121.40 (C-13), 124.75 (C-19), 124.91 (C-17), 127.17 (C-18), 132.54 (C-14), 133.03 (C-12), 148.47 (C-16), 157.55 (C-10), 165.48 (C-8), 210.80 (C-4). HRMS (ESI+): *m/z* calcd for $[M + H]^+$ 344.1315; found 344.1304. HPLC purity, 98.8% at 254 nm (t_R = 4.41 min).

4.3.11. N-(((1S,4S)-4-Hydroxy-1-(thiophen-2-yl)cyclohexyl)methyl) furan-3-carboxamide (cis-15)

Synthesized from **9** (606 mg, 2.0 mmol, 1.0 equiv) and $NaBH_4$ (151 mg, 4.0 mmol, 2.0 equiv) via general procedure H. Column chromatography, DCM/diethyl ether = 2/1 (v/v). Yield: 34% (205 mg); white solid. ^{1}H NMR (400 MHz, DMSO-d_6): δ_H 1.15–1.28 (2H, m, H_a-3,5), 1.57–1.67 (2H, m, H_a-2,6), 1.65–1.72 (2H, m, H_e-3,5), 1.99–2.08 (2H, m, H_e-2,6), 3.23 (2H, d, J = 6.4 Hz, H-7′, H-7′′), 3.34–3.40 (1H, m, H-4), 4.41 (1H, brs, OH), 6.82 (1H, dd, J_1 = 1.7 Hz, J_2 = 0.8 Hz, H-12), 6.93 (1H, dd, J_1 = 3.5 Hz, J_2 = 1.1 Hz, H-14), 6.99 (1H, dd, J_1 = 5.1 Hz, J_2 = 3.5 Hz, H-15), 7.40 (1H, dd, J_1=5.1 Hz, J_2 = 1.1 Hz, H-16), 7.69 (1H, t, J = 1.7 Hz, H-11), 7.93 (1H, brt, J = 6.4 Hz, NHCO), 8.16 (1H, dd, J_1 = 1.7 Hz, J_2 = 0.8 Hz, H-10). ^{13}C NMR (101 MHz, DMSO-d_6): δ_C 31.19 (C-3,5), 32.60 (C-2,6), 42.66 (C-1), 51.15 (C-7), 68.48 (C-4), 109.16 (C-12), 122.75 (C-9), 124.07 (C-16), 124.27 (C-14), 126.98 (C-15), 143.79 (C-11), 145.01 (C-10), 149.53 (C-13), 161.75 (C-8). HRMS (ESI+): *m/z* calcd for $[M + H]^+$ 306.1158; found 306.1149. HPLC purity, 99.8% at 254 nm (t_R = 2.94 min).

4.3.12. N-(((1R,4R)-4-Hydroxy-1-(thiophen-2-yl)cyclohexyl)methyl) furan-3-carboxamide (trans-15)

Synthesized from **9** (606 mg, 2.0 mmol, 1.0 equiv) and $NaBH_4$ (151 mg, 4.0 mmol, 2.0 equiv) via general procedure H. Column chromatography, DCM/diethyl ether = 2/1 (v/v). Yield: 42% (254 mg); white solid. ^{1}H NMR (400 MHz, DMSO-d_6): δ_H 1.37–1.63 (4H, m, H_a-3,5, H_e-3,5), 1.64–1.72 (2H, m, H_a-2,6), 2.00–2.06 (2H, m, H_e-2,6), 3.32 (2H, d, J = 6.5 Hz, H-7′, H-7′′), 3.60 (1H, brs, H-4), 4.39 (1H, s, OH), 6.81 (1H, s, H-12), 6.90 (1H, d, J = 3.5 Hz, H-14), 6.96 (1H, dd, J_1=5.0 Hz, J_2 = 3.5 Hz, H-15), 7.36 (1H, d, J = 5.0 Hz, H-16), 7.68 (1H, s, H-11), 7.81 (1H, brt, J = 6.5 Hz, NHCO), 8.14 (1H, s, H-10). ^{13}C NMR (101 MHz, DMSO-d_6): δ_C 29.49 (C-3,5), 29.91 (C-2,6), 42.26 (C-1), 49.57 (C-7), 64.77 (C-4), 109.19 (C-12), 122.80 (C-9), 123.73 (C-16), 123.84 (C-14), 126.68 (C-15), 143.75 (C-11), 144.98 (C-10), 150.46 (C-13), 161.70 (C-8). HRMS (ESI+): *m/z* calcd for $[M + H]^+$ 306.1158; found 306.1149. HPLC purity, 95.5% at 254 nm (t_R = 3.45 min).

4.3.13. 5-Fluoro-N-(((1S,4S)-4-hydroxy-1-(thiophen-2-yl)cyclohexyl) methyl)-2-methoxybenzamide (cis-16)

Synthesized from **8** (761 mg, 2.1 mmol, 1.0 equiv) and $NaBH_4$ (160 mg, 4.2 mmol, 2.0 equiv) via general procedure H. Column chromatography, EtOAc/*n*-hexane = 1/2 (v/v). Yield: 16% (120 mg); white solid. ^{1}H NMR (400 MHz, DMSO-d_6): δ_H 1.20–1.34 (2H, m, H_a-3,5), 1.55–1.67 (2H, m, H_a-2,6), 1.67–1.76 (2H, m, H_e-3,5), 2.05–2.13 (2H, m, H_e-2,6, H_e-3,5), 3.41 (2H, d, J = 6.0 Hz, H-7′, H-7′′), 3.43–3.51 (1H, m, H-4), 3.78 (3H, s, OCH_3), 4.46 (1H, d, J = 4.6 Hz, OH), 7.02 (1H, dd, J_1 = 3.5 Hz, J_2 = 1.1 Hz, H-17), 7.08 (1H, dd, J_1 = 5.1 Hz, J_2 = 3.5 Hz, H-18), 7.16 (1H, dd, J_1 = 9.1 Hz, J_2 = 4.3 Hz, H-11), 7.33 (1H, ddd, J_1 = 9.1 Hz, J_2 = 7.8 Hz, J_3 = 3.3 Hz, H-12), 7.48 (1H, dd, J_1 = 5.1 Hz, J_2 = 1.1 Hz, H-19), 7.54 (1H, dd, J_1 = 9.4 Hz, J_2 = 3.3 Hz, H-14), 7.93 (1H, brt, J = 6.0 Hz, CONH). ^{13}C NMR (101 MHz, DMSO-d_6): δ_C 30.93 (C-3,5), 32.57 (C-2,6), 41.72 (C-1), 51.77 (C-7), 56.51 (C-15), 68.07 (C-4), 114.00 (d, J = 7.7 Hz, C-11), 116.63 (d, J = 24.7 Hz, C-14), 118.73 (d, J = 23.0 Hz, C-12), 123.32 (d, J = 6.5 Hz, C-9), 124.46 (C-19), 124.65 (C-17), 127.09 (C-18), 149.55 (C-16), 153.39 (d, J = 1.7 Hz, C-10), 156.04 (d, J = 236.9 Hz, C-13), 163.26 (d, J = 1.8 Hz, C-8). HRMS (ESI+): *m/z* calcd for $[M + H]^+$ 364.1377; found 364.1365. HPLC purity, 95.4% at 254 nm (t_R = 4.33 min).

4.3.14. 5-Fluoro-N-(((1R,4R)-4-hydroxy-1-(thiophen-2-yl)cyclohexyl) methyl)-2-methoxybenzamide (trans-16)

Synthesized from **8** (761 mg, 2.1 mmol, 1.0 equiv) and $NaBH_4$ (160 mg, 4.2 mmol, 2.0 equiv) via general procedure H. Column chromatography, EtOAc/*n*-hexane = 1/2 (v/v). Yield: 24% (180 mg); white solid. ^{1}H NMR (400 MHz, DMSO-d_6): δ_H 1.48–1.64 (4H, m, H_e-3,5, H_a-3,5), 1.67–1.76 (2H, m, H_a-2,6), 1.92–2.03 (2H, m, H_e-2,6), 3.51–3.61 (3H, m, H-7′, H-7′′, H-4), 3.72 (3H, s, OCH_3), 4.52 (1H, d, J = 3.9 Hz, OH), 7.00 (1H, dd, J_1 = 3.5 Hz, J_2 = 1.1 Hz, H-17), 7.06 (1H, dd, J_1 = 5.1 Hz, J_2 = 3.5 Hz, H-18), 7.14 (1H, dd, J_1 = 9.2 Hz, J_2 = 4.3 Hz, H-11), 7.33 (1H, ddd, J_1 = 9.2 Hz, J_2 = 7.7 Hz, J_3 = 3.4 Hz, H-12), 7.46 (1H, dd, J_1 = 5.1 Hz, J_2 = 1.1 Hz, H-19), 7.58 (1H, dd, J_1 = 9.5 Hz, J_2 = 3.4 Hz, H-14), 7.87 (1H, brt, J = 5.9 Hz, CONH). ^{13}C NMR (101 MHz, DMSO-d_6): δ_C 29.96 (C-3,5), 31.21 (C-2,6), 41.05 (C-1), 48.76 (C-7), 56.46 (C-15), 66.00 (C-4), 114.08 (d, J = 7.9 Hz, C-11), 116.75 (d, J = 24.8 Hz, C-14), 118.91 (d, J = 23.1 Hz, C-12), 122.88 (d, J = 6.4 Hz, C-9), 123.98 (C-19), 124.13 (C-17), 126.88 (C-18), 151.09 (C-16), 153.47 (d, J = 1.7 Hz, C-10), 156.07 (d, J = 237.0 Hz, C-13), 163.05 (d, J = 1.7 Hz, C-8). HRMS (ESI+): *m/z* calcd for $[M + H]^+$ 364.1377; found 364.1364. HPLC purity, 95.3% at 254 nm (t_R = 4.62 min).

4.3.15. N-(((1R,4R)-4-Hydroxy-1-(thiophen-3-yl)cyclohexyl)methyl)-2-methoxybenzamide (trans-17)

Note: H_a corresponds to axial protons and H_e to equatorial protons.

Synthesized from **22** (5.90 g, 17.0 mmol, 1.0 equiv) and $NaBH_4$ (1.29 g, 34.0 mmol, 2.0 equiv) via general procedure H. Column chromatography, DCM/diethyl ether = 2/1 (v/v). Yield: 34% (2.0 g); white solid. ^{1}H NMR (400 MHz, DMSO-d_6): δ_H 1.10–1.25 (2H, m, H_a-3,5), 1.45–1.57 (2H, m, H_a-2,6), 1.62–1.75 (2H, m, H_e-3,5), 2.10–2.20 (2H, m, H_e-2,6), 3.38 (2H, d, J = 5.7 Hz, H-7′, H-7′′), 3.42–3.51 (1H, m, H-4), 3.78 (3H, s, OCH_3), 4.40 (1H, d, J = 4.5 Hz, OH), 7.02 (1H, td, J_1 = 7.7 Hz, J_2 = 1.0 Hz, H-13), 7.11 (1H, dd, J_1 = 8.4 Hz, J_2 = 0.9 Hz, H-11), 7.17 (1H, dd, J_1 = 5.0 Hz, J_2 = 1.4 Hz, H-18), 7.37 (1H, dd, J_1 = 2.9 Hz, J_2 = 1.4 Hz, H-16), 7.46 (1H, ddd, J_1 = 8.3 Hz, J_2 = 7.3 Hz, J_3 = 1.9 Hz, H-12), 7.57 (1H, dd, J_1 = 5.0 Hz, J_2 = 2.9 Hz, H-19), 7.69 (1H, brt, J = 5.7 Hz, NHCO), 7.84 (1H, dd, J_1 = 7.7 Hz, J_2 = 1.9 Hz, H-14). ^{13}C NMR (101 MHz, DMSO-d_6): δ_C 31.02 (C-3,5), 31.66 (C-2,6), 40.77 (C-1), 50.55 (C-7), 55.88 (C-15), 68.43 (C-4), 112.08 (C-11), 120.65 (C-13), 121.65 (C-16), 121.71 (C-9), 126.21 (C-19), 126.77 (C-18), 130.90 (C-14), 132.52 (C-12), 145.78 (C-17), 157.06 (C-10), 164.27 (C-8). HRMS (ESI+): *m/z* calcd for $[M + H]^+$ 346.1471; found 346.1459. HPLC purity, 98.2% at 254 nm (t_R = 3.84 min).

4.3.16. N-(((1S,4S)-4-Hydroxy-1-(thiophen-3-yl)cyclohexyl)methyl)-2-methoxybenzamide (cis-17)

Synthesized from **22** (5.90 g, 17.0 mmol, 1.0 equiv) and $NaBH_4$ (1.29 g, 34.0 mmol, 2.0 equiv) via general procedure H. Column chromatography, DCM/diethyl ether = 2/1 (v/v). Yield: 57% (3.3 g); white solid. ^{1}H NMR (400 MHz, DMSO-d_6): δ_H 1.46–1.61 (4H, m, H_a-3,5, H_e-3,5), 1.62–1.72 (2H, m, H_a-2,6), 1.89–1.99 (2H, m, H_e-2,6), 3.46–3.54 (1H, m, H-4), 3.59 (2H, d, J = 5.8 Hz, H-7′, H-7′′), 3.71 (3H, s, OCH_3), 4.50 (1H, d, J = 4.0 Hz, OH), 7.03 (1H, td, J_1 = 7.5 Hz, J_2 = 1.0 Hz, H-13), 7.09 (1H, dd, J_1 = 8.4 Hz, J_2 = 1.0 Hz, H-11), 7.20 (1H, dd, J_1 = 5.0 Hz, J_2 = 1.4 Hz, H-18), 7.33 (1H, dd, J_1 = 2.9 Hz, J_2 = 1.4 Hz, H-16), 7.46 (1H, ddd, J_1 = 8.4 Hz, J_2 = 7.3 Hz, J_3 = 1.9 Hz, 1H, H-12), 7.57 (1H, dd, J_1 = 5.0 Hz, J_2 = 2.9 Hz, H-19), 7.62 (1H, brt, J = 5.7 Hz, NHCO), 7.89 (1H, dd, J_1 = 7.8 Hz, J_2 = 1.9 Hz, H-14). ^{13}C NMR (101 MHz, DMSO-d_6): δ_C 30.22 (C-3,5), 30.50 (C-2,6), 39.86 (C-1), 46.77 (C-7), 55.80 (C-15), 66.74 (C-4), 112.11 (C-11), 120.70 (C-13, C-16), 121.24 (C-9), 126.14 (C-19), 126.51 (C-18), 131.06 (C-14), 132.66 (C-12), 147.81 (C-17), 157.11 (C-10), 164.04 (C-8). HRMS (ESI+): *m/z* calcd for $[M + H]^+$ 346.1471; found 346.1459. HPLC purity, 96.1% at 254 nm (t_R = 4.31 min).

4.3.17. (1R,4R)-4-((2-Methoxybenzamido)methyl)-4-(thiophen-3-yl) cyclohexyl propylcarbamate (trans-18)

Synthesized from *trans*-**17** (103 mg, 0.30 mmol, 1 equiv), 4-nitrophenyl chloroformate (121 mg, 0.60 mmol, 2 equiv), Et_3N (0.13 mL, 0.90 mmol, 3 equiv) and propyl amine (0.25 mL, 3 mmol, 10 equiv) via general procedure I. Column chromatography, ethylacetate (EtOAc)/*n*-hexane = 1/1 (v/v). Two conformers in a 15:85 ratio. Yield: 50% (60 mg); white solid. ^{1}H NMR (400 MHz, $CDCl_3$) for both conformers: δ 0.88 (3H, t, J = 7.0 Hz, H-23′, H-23′′, H-23‴), 1.40–1.55 (4H, m, H-22′, H-

22'', H_a-3,5), 1.68–1.76 (2H, m, H_a-2,6), 1.89–1.97 (2H, m, H_e-3,5), 2.15–2.23 (2H, m, H_e-2,6), 3.09 (2H, dd, J_1 = 13.0 Hz, J_2 = 6.5 Hz, H-21′, H-21''), 3.60 (2H, d, J = 5.2 Hz, H-7′, H-7''), 3.74 (3H, s, OCH$_3$), 4.63 (1H, brs, OCH$_2$NHCO), 4.71 (1H, brs, H-4), 6.90 (1H, dd, J_1=8.3 Hz, J_2 = 3.4 Hz, H-11), 7.01–7.08 (1H, m, H-13), 7.10–7.14 (2H, m, H-18, H-16), 7.35–7.45 (2H, m, H-12, H-19), 7.66 (1H, t, J = 5.5 Hz, CH$_2$NHCO), 8.19 (1H, dd, J_1=7.8 Hz, J_2 = 1.7 Hz, H-14). ^{13}C NMR (101 MHz, $CDCl_3$) for both conformers: δ 11.29 (C-23), 23.28 (C-22), 27.57 (C-3,5), 31.71 (C-2,6), 41.01 (C-1), 42.67 (C-21), 50.20 (C-7), 55.67 (C-15), 72.47 (C-4), 111.20 (C-11), 121.23 (C-13), 121.30 (C-9, C-16), 126.09 (C-19), 126.48 (C-18), 132.50 (C-14), 132.80 (C-12), 146.17 (C-17), 156.23 (C-20), 157.51 (C-10), 165.32 (C-8). HRMS (ESI+): *m/z* calcd for $[M + H]^+$ 431.1999; found 431.1981. HPLC purity, 99.1% at 254 nm (t_R = 5.48 min).

4.3.18. (1S,4S)-4-((2-Methoxybenzamido)methyl)-4-(thiophen-3-yl) cyclohexyl propylcarbamate (cis-18)

Synthesized from *cis*-**17** (103 mg, 0.30 mmol, 1 equiv), 4-nitrophenyl chloroformate (121 mg, 0.60 mmol, 2 equiv), Et_3N (0.13 mL, 0.90 mmol, 3 equiv) and propyl amine (0.25 mL, 3 mmol, 10 equiv) via general procedure I. Column chromatography, EtOAc/*n*-hexane = 1/1 (v/v). Two conformers in a 12:88 ratio. Yield: 47% (63 mg); white solid. ^{1}H NMR (400 MHz, $CDCl_3$) for both conformers: δ 0.93 (3H, t, J = 7.4 Hz, H-23′, H-23'', H-23'''), 1.47–1.59 (2H, m, H-22′, H-22''), 1.65–1.75 (2H, m, H_a-3,5), 1.76–1.86 (2H, m, H_e-3,5), 1.88–2.04 (4H, m, H_e-2,6, H_a-2,6), 3.14 (2H, dd, J_1=13.4 Hz, J_2 = 6.7 Hz, H-21′, H-21''), 3.70 (2H, d, J = 6.8 Hz, H-7′, H-7''), 3.71 (3H, s, OCH$_3$), 4.73 (brs, 2H, OCH$_2$NHCO, H-4), 6.89 (1H, d, J = 8.2 Hz, H-11), 7.02–7.08 (1H, m, H-13), 7.09–7.16 (2H, m, H-18, H-16), 7.35–7.45 (2H, m, H-12, H-19), 7.64 (1H, brs, CONHCH$_2$), 8.21 (1H, dd, J_1=7.8 Hz, J_2 = 1.8 Hz, H-14). ^{13}C NMR (100 MHz, $CDCl_3$) for both conformers: δ 11.39 (C-23), 23.38 (C-22), 27.07 (C-3,5), 30.56 (C-2,6), 40.77 (C-1), 42.75 (C-21), 49.16 (C-7), 55.63 (C-15), 70.89 (C-4), 111.22 (C-11), 120.98 (C-16), 121.32 (C-13, C-9), 126.04 (C-19), 126.48 (C-18), 132.56 (C-14), 132.80 (C-12), 146.81 (C-17), 156.38 (C-20), 157.57 (C-10), 165.32 (C-8). HRMS (ESI+): *m/z* calcd for $[M + H]^+$ 431.1999; found 431.1987. HPLC purity, 95.5% at 254 nm (t_R = 5.51 min).

4.3.19. (1R,4R)-4-((2-Methoxybenzamido)methyl)-4-(thiophen-3-yl) cyclohexyl methylcarbamate (trans-19)

Synthesized from *trans*-**17** (103 mg, 0.30 mmol, 1 equiv), 4-nitrophenyl chloroformate (121 mg, 0.60 mmol, 2 equiv), Et_3N (0.13 mL, 0.90 mmol, 3 equiv) and methyl amine (93 mg, 3 mmol, 10 equiv) via general procedure I. Column chromatography, EtOAc/*n*-hexane = 1/1 (v/v). Two conformers in a 9:91 ratio. Yield: 47% (58 mg); white solid. ^{1}H NMR (400 MHz, DMSO-d_6) for both conformers: δ_H 1.25–1.38 (2H, m, H_a-3,5), 1.59–1.69 (2H, m, H_a-2,6), 1.74–1.84 (2H, m, H_e-3,5), 2.12–2.17 (2H, m, H_e-2,6), 2.52 (3H, d, J = 4.6 Hz, NHCH$_3$), 3.43 (2H, d, J = 5.8 Hz, H-7′, H-7''), 3.77 (3H, s, OCH$_3$), 4.50–4.60 (1H, m, H-4), 6.82 (1H, q, J = 4.6 Hz, CONHCH$_3$), 7.02 (1H, ddd, J_1 = 7.7 Hz, J_2 = 7.3 Hz, J_3 = 1.0 Hz, H-13), 7.10 (1H, dd, J_1 = 8.3 Hz, J_2 = 1.0 Hz, H-11), 7.19 (1H, d, J_1 = 5.0 Hz, J_2 = 0.9 Hz, H-18), 7.40 (dd, J_1 = 2.6 Hz, J_2 = 1.1 Hz, H-16), 7.46 (1H, ddd, J_1 = 8.3 Hz, J_2 = 7.3 Hz, J_3 = 1.9 Hz, H-12), 7.59 (1H, dd, J_1 = 5.0 Hz, J_2 = 2.9 Hz, H-19), 7.72 (1H, brt, J = 5.8 Hz, NHCO), 7.83 (1H, dd, J_1 = 7.7 Hz, J_2 = 1.9 Hz, H-14). ^{13}C NMR (101 MHz, DMSO-d_6) for both conformers: δ_C 26.79 (C-21), 27.46 (C-3,5), 31.05 (C-2,6), 40.62 (C-1), 49.68 (C-7), 55.84 (C-15), 71.32 (C-4), 112.05 (C-11), 120.63 (C-13), 121.68 (C-9), 121.81 (C-16), 126.37 (C-19), 126.65 (C-18), 130.84 (C-14), 132.49 (C-12), 145.63 (C-17), 156.25 (C-20), 157.02 (C-10), 164.38 (C-8). HRMS (ESI+): *m/z* calcd for $[M + H]^+$ 403.1686; found 403.1669. HPLC purity, 100.0% at 254 nm (t_R = 4.71 min).

4.3.20. (1S,4S)-4-((2-Methoxybenzamido)methyl)-4-(thiophen-3-yl) cyclohexyl methylcarbamate (cis-19)

Synthesized from *cis*-**17** (215 mg, 0.6 mmol, 1 equiv), 4-nitrophenyl chloroformate (242 mg, 1.2 mmol, 2 equiv), Et_3N (0.25 mL, 1.8 mmol, 3 equiv) and methyl amine (186 mg, 6 mmol, 10 equiv) via general procedure I. Column chromatography, EtOAc/*n*-hexane = 1/1 (v/v). Two conformers in a 12:88 ratio. Yield: 42% (106 mg); white solid. ^{1}H NMR (400 MHz, DMSO-d_6) for both conformers: δ_H 1.54–1.74 (4H, m, H_e-3,5, H_a-3,5), 1.75–2.04 (4H, m, H_e-2,6, H_a-2,6), 2.56 (3H, d, J = 4.5 Hz, NHCH$_3$), 3.58 (2H, d, J = 5.8 Hz, H-7′, H-7''), 3.71 (3H, s, OCH$_3$), 4.52–4.60 (1H, m, H-4), 6.96 (1H, q, J = 4.5 Hz, CONHCH$_3$), 7.03 (1H, ddd, J_1 = 7.7 Hz, J_2 = 7.2 Hz, J_3 = 1.0 Hz, H-13), 7.09 (1H, dd, J_1 = 8.4 Hz, J_2 = 1.0 Hz, H-11), 7.22 (1H, dd, J_1 = 5.0 Hz, J_2 = 1.3 Hz, H-18), 7.37 (1H, dd, J_1 = 2.9 Hz, J_2 = 1.3 Hz, H-16), 7.46 (1H, ddd, J_1 = 8.4 Hz, J_2 = 7.2 Hz, J_3 = 1.9 Hz, H-12), 7.59 (1H, dd, J_1 = 5.0 Hz, J_2 = 2.9 Hz, H-19), 7.63 (1H, brt, J = 5.8 Hz, CH$_2$NHCO), 7.89 (1H, dd, J_1 = 7.7 Hz, J_2 = 1.9 Hz, H-14). ^{13}C NMR (101 MHz, DMSO-d_6) for both conformers: δ_C 26.85 (C-21), 26.92 (C-3,5), 30.22 (C-2,6), 39.91 (C-1), 47.31 (C-7), 55.82 (C-15), 70.02 (C-4), 112.12 (C-11), 120.69 (C-13), 121.07 (C-16), 121.20 (C-9), 126.31 (C-19), 126.53 (C-18), 131.05 (C-14), 132.69 (C-12), 146.83 (C-17), 156.32 (C-20), 157.12 (C-10), 164.13 (C-8). HRMS (ESI+): *m/z* calcd for $[M + H]^+$ 403.1686; found 403.1682. HPLC purity, 99.6% at 254 nm (t_R = 4.79 min).

4.3.21. (1R,4R)-4-((2-Methoxybenzamido)methyl)-4-(thiophen-3-yl) cyclohexyl allylcarbamate (trans-20)

Synthesized from *trans*-**17** (103 mg, 0.30 mmol, 1 equiv), 4-nitrophenyl chloroformate (121 mg, 0.60 mmol, 2 equiv), Et_3N (0.13 mL, 0.90 mmol, 3 equiv) and 2-propen-1-amine (0.22 mL, 3 mmol, 10 equiv) via general procedure I. Column chromatography, EtOAc/*n*-hexane = 1/1 (v/v). Two conformers in a 15:85 ratio. Yield: 50% (64 mg); white solid. ^{1}H NMR (400 MHz, $CDCl_3$) for both conformers: δ 1.44–1.59 (2H, m, H_a-3,5), 1.66–1.80 (2H, m, H_a-2,6), 1.89–1.99 (2H, m, H_e-3,5), 2.15–2.24 (2H, m, H_e-2,6), 3.61 (2H, d, J = 6.0 Hz, H-7′, H-7''), 3.74 (3H, s, OCH$_3$), 3.75 (2H, brs, H-21′, H-21''), 4.63 (1H, brs, OCH$_2$NHCO), 4.74 (1H, brs, H-4), 5.12 (2H, dd, J_1 = 22.7 Hz, J_2 = 13.7 Hz, H-23′, H-23''), 5.72–5.88 (1H, m, H-22), 6.90 (1H, d, J = 8.3 Hz, H-11), 7.01–7.08 (1H, m, H-13), 7.09–7.14 (2H, m, H-18, H-16), 7.36–7.44 (2H, m, H-12, H-19), 7.65 (1H, t, J = 5.5 Hz, NHCO), 8.20 (1H, dd, J_1=7.8 Hz, J_2 = 1.8 Hz, H-14). ^{13}C NMR (101 MHz, $CDCl_3$) for both conformers: δ 27.57 (C-3,5), 31.71 (C-2,6), 41.06 (C-1), 43.45 (C-21), 50.20 (C-7), 55.70 (C-15), 72.82 (C-4), 111.22 (C-11), 116.03 (C-23), 121.32 (C-13, C-9), 121.36 (C-16), 126.12 (C-19), 126.52 (C-18), 132.58 (C-14), 132.81 (C-12), 134.74 (C-22), 146.27 (C-17), 156.06 (C-20), 157.54 (C-10), 165.32 (C-8). HRMS (ESI+): *m/z* calcd for $[M + H]^+$ 429.1843; found 429.1838. HPLC purity, 98.2% at 254 nm (t_R = 5.27 min).

4.3.22. (1S,4S)-4-((2-Methoxybenzamido)methyl)-4-(thiophen-3-yl) cyclohexyl (3-methoxypropyl)carbamate (cis-21)

Synthesized from *cis*-**17** (103 mg, 0.3 mmol, 1.0 equiv), 4-nitrophenyl chloroformate (121 mg, 0.6 mmol, 2.0 equiv), Et_3N (0.13 mL, 0.9 mmol, 3.0 equiv) and 3-methoxypropylamine (0.31 mL, 3.0 mmol, 10.0 equiv) via general procedure I. Column chromatography, EtOAc/*n*-hexane = 1/1 (v/v). Two conformers in a 11:89 ratio. Yield: 48% (67 mg); white solid. ^{1}H NMR (400 MHz, DMSO-d_6) for both conformers: δ 1.57–1.73 (6H, m, H-22′, H-22'', H_a-3,5, H_e-3,5), 1.75–1.96 (4H, m, H_e-2,6, H_a-2,6), 3.01 (2H, dd, J_1 = 12.9 Hz, J_2 = 6.6 Hz, H-21′, H-21''), 3.21 (3H, s, H-24′, H-24'', H-24'''), 3.28–3.34 (2H, m, H-23′, H-23''), 3.59 (2H, d, J = 5.6 Hz, H-7′, H-7''), 3.72 (3H, s, OCH$_3$), 4.56 (1H, brs, H-4), 7.01–7.06 (1H, m, H-13), 7.06–7.14 (2H, m, H-11, OCONHCH$_2$), 7.22 (1H, dd, J_1=5.0 Hz, J_2 = 1.3 Hz, H-18), 7.37 (1H, d, J = 1.5 Hz, H-16), 7.46 (1H, ddd, J_1=9.0 Hz, J_2=7.4 Hz, J_3=1.9 Hz, H-12), 7.59 (1H, dd, J_1=5.0 Hz, J_2=2.9 Hz, H-19), 7.64 (1H, t, J = 5.5 Hz, CONHCH$_2$), 7.89 (1H, dd, J_1=7.8 Hz, J_2=1.8 Hz, H-14). ^{13}C NMR (100 MHz, DMSO-d_6) for both conformers: δ 26.91 (C-3,5), 29.56 (C-22), 30.23 (C-2,6), 37.41 (C-21), 40.33 (C-1), 47.33 (C-7), 55.83 (C-15), 57.89 (C-24), 69.51 (C-23), 70.00 (C-4), 112.14 (C-11), 120.71 (C-13), 121.08 (C-16), 121.23 (C-9), 126.33 (C-19), 126.54 (C-18), 131.07 (C-14), 132.71 (C-12),

146.87 (C-17), 155.81 (C-20), 157.14 (C-10), 164.15 (C-8). HRMS (ESI+): *m/z* calcd for $[M + H]^+$ 461.2105; found 461.2104. HPLC purity, 100% at 254 nm ($t_R = 5.08$ min).

4.3.23. 2-Methoxy-N-((4-oxo-1-(thiophen-3-yl)cyclohexyl)methyl) benzamide (22)

Synthesized from **33** (8.90 g, 23.0 mmol, 1.0 equiv), pyridinium *p*-toluenesulfonate (0.58 g, 2.3 mmol, 0.1 equiv) and water (20 mL) via general procedure G. Column chromatography, EtOAc/*n*-hexane = 1/1 (v/v). Yield: 75% (5.90 g); white solid. ^{1}H NMR (400 MHz, $CDCl_3$): δ 2.08–2.18 (2H, m, H_a-2,6), 2.30–2.44 (4H, m, H_a-3,5, H_e-2,6), 2.45–2.54 (2H, m, H_e-3,5), 3.75 (3H, s, OCH_3), 3.76 (2H, d, $J = 7.0$ Hz, H-7′, H-7′′), 6.92 (1H, d, $J = 8.3$ Hz, H-11), 7.06 (1H, t, $J = 7.6$ Hz, H-13), 7.18 (1H, dd, J_1=5.0 Hz, J_2=1.3 Hz, H-18), 7.21 (1H, dd, J_1=2.9 Hz, J_2=1.4 Hz, H-16), 7.39–7.48 (2H, m, H-12, H-19), 7.75 (1H, t, $J = 5.3$ Hz, NHCO), 8.20 (1H, dd, J_1=7.8 Hz, J_2=1.8 Hz, H-14). ^{13}C NMR (100 MHz, $CDCl_3$): δ 34.15 (C-2,6), 37.80 (C-3,5), 41.18 (C-1), 49.28 (C-7), 55.70 (C-15), 111.24 (C-11), 121.01 (C-9), 121.39 (C-13), 121.61 (C-16), 126.24 (C-18), 126.79 (C-19), 132.53 (C-14), 133.00 (C-12), 144.68 (C-17), 157.51 (C-10), 165.43 (C-8), 211.14 (C-4). HRMS (ESI+): *m/z* calcd for $[M + H]^+$ 344.1315; found 344.1307. HPLC purity, 99.5% at 254 nm (t_R = 4.33 min).

4.3.24. (1R,4R)-4-((2-Methoxybenzamido)methyl)-4-(thiophen-3-yl) cyclohexan-1-aminium chloride (trans-23)

Synthesized from *cis*-**17** (691 mg, 2.0 mmol, 1.0 equiv), Et_3N (0.56 mL, 4.0 mmol, 2.0 equiv), methanesulfonyl chloride (0.31 mL, 4.0 mmol, 2.0 equiv) and sodium azide (0.26 g, 4.0 mmol, 2.0 equiv) via general procedure J, Pd/C (50 mg) via general procedure K, and 4 M HCl solution (3 mmol, 10 equiv) via general procedure L. Column chromatography, Biotage Isolera One System reversed-phase chromatography (Biotage SNAP Cartridge KP-C18-HS 12 g column), MF: gradient water in H_2O/acetonitrile. Yield: 17% (50 mg); white solid. ^{1}H NMR (400 MHz, DMSO-d_6): δ_H 1.24–1.36 (2H, m, H_a-3,5), 1.54–1.65 (2H, m, H_a-2,6), 1.80–1.90 (2H, m, H_e-3,5), 2.24–2.35 (2H, m, H_e-2,6), 2.91–3.06 (1H, m, H-4), 3.35 (2H, d, $J = 5.7$ Hz, H-7′, H-7′′), 3.80 (3H, s, OCH_3), 7.03 (1H, t, $J = 7.6$ Hz, H-13), 7.12 (1H, d, $J = 8.3$ Hz, H-11), 7.19 (1H, d, $J = 5.1$ Hz, H-18), 7.39–7.50 (2H, m, H-12, H-16), 7.58–7.64 (1H, m, H-19), 7.73 (1H, brt, $J = 5.7$ Hz, NHCO), 7.82 (1H, d, $J = 7.6$ Hz, H-14), 7.93 (3H, brs, $CHNH_3^+$). ^{13}C NMR (101 MHz, DMSO-d_6): δ_C 26.46 (C-3,5), 31.64 (C-2,6), 40.85 (C-1), 49.47 (C-4), 51.31 (C-7), 55.91 (C-15), 112.07 (C-11), 120.63 (C-13), 121.89 (C-9), 122.19 (C-16), 126.52 (C-19), 126.80 (C-18), 130.81 (C-14), 132.49 (C-12), 144.43 (C-17), 157.02 (C-10), 164.47 (C-8). HRMS (ESI+): *m/z* calcd for $[M + H]^+$ 345.1631; found 345.1627. HPLC purity, 97.7% at 254 nm ($t_R = 2.79$ min).

4.3.25. (1S,4S)-4-((2-Methoxybenzamido)methyl)-4-(thiophen-3-yl) cyclohexan-1-aminium chloride (cis-23)

Synthesized from *trans*-**17** (691 mg, 2.0 mmol, 1.0 equiv), Et_3N (0.56 mL, 4.0 mmol, 2.0 equiv), methanesulfonyl chloride (0.31 mL, 4.0 mmol, 2.0 equiv) and sodium azide (0.26 g, 4.0 mmol, 2.0 equiv) via general procedure J, Pd/C (40 mg) via general procedure K, and 4 M HCl solution (3 mmol, 10 equiv) via general procedure L. Column chromatography, Biotage Isolera One System reversed-phase chromatography (Biotage SNAP Cartridge KP-C18-HS 12 g column), MF: gradient water in H_2O/acetonitrile. Yield: 18% (48 mg); white solid. ^{1}H NMR (400 MHz, DMSO-d_6): δ_H 1.60–1.70 (2H, m, H_a-2,6), 1.70–1.88 (4H, m, H_e-3,5, H_a-3,5), 1.98–2.06 (2H, m, H_e-2,6), 3.05 (1H, brs, H-4), 3.66 (3H, s, OCH_3), 3.72 (2H, d, $J = 5.8$ Hz, H-7′, H-7′′), 7.03 (1H, ddd, $J_1 = 7.8$ Hz, $J_2 = 7.2$ Hz, $J_2 = 1.0$ Hz, H-13), 7.08 (1H, dd, J_1=8.5 Hz, $J_2 = 1.0$ Hz, H-11), 7.24 (1H, dd, $J_1 = 5.1$ Hz, $J_2 = 1.4$ Hz, H-18), 7.35 (1H, dd, $J_1 = 2.9$ Hz, $J_2 = 1.4$ Hz, H-16), 7.46 (1H, ddd, $J_1 = 8.5$ Hz, $J_2 = 7.2$ Hz, $J_3 = 1.8$ Hz, H-12), 7.58 (1H, brt, $J = 5.8$ Hz, NHCO), 7.60 (1H, dd, $J_1 = 5.1$ Hz, $J_2 = 2.9$ Hz, H-19), 7.90 (1H, dd, $J_1 = 7.8$ Hz, $J_2 = 1.8$ Hz, H-14), 8.13 (3H, s, $CHNH_3^+$). ^{13}C NMR (101 MHz, DMSO-d_6): δ_C 25.64 (C-3,5), 31.05 (C-2,6), 39.15 (C-1), 44.18 (C-7), 48.53 (C-4), 55.77 (C-15), 112.16 (C-11), 120.53 (C-9), 120.73 (C-16), 121.06 (C-13), 126.23 (C-18), 126.40 (C-19), 131.05 (C-14), 132.78 (C-12), 148.32 (C-17), 157.11 (C-10), 164.11 (C-8). HRMS (ESI+): *m/z* calcd for $[M + H]^+$ 345.1631; found 345.1627. HPLC purity, 98.7% at 254 nm ($t_R = 3.67$ min).

4.3.26. Methyl 5-cyano-2-oxo-5-(thiophen-2-yl)cyclohexane-1-carboxylate (24)

Synthesized from 2-(thiophen-2-yl)acetonitrile (10.60 mL, 100.0 mmol, 1.0 equiv), methyl acrylate (45.30 mL, 500.0 mmol, 5.0 equiv) and benzyltrimethylammonium hydroxide (17.60 mL, 100.0 mmol, 1.0 equiv.) via general procedure A and potassium *tert*-butoxide (17.95 g, 160.0 mmol, 2 equiv) via general procedure B. The product was used without further purification. Yield: 48% (12.60 g); pale yellow solid. ^{1}H NMR (400 MHz, DMSO-d_6): δ 2.22–2.31 (m, 1H), 2.39–2.49 (m, 2H), 2.52–2.67 (m, 2H), 2.77 (dd, $J_1 = 15.7$ Hz, $J_2 = 1.0$ Hz, 1H), 3.03 (d, J = 16.1 Hz, 1H), 3.76 (s, 3H), 7.08 (dd, J_1=5.1 Hz, J_2=3.6 Hz, 1H), 7.27 (dd, J_1=3.6 Hz, J_2=1.2 Hz, 1H), 7.59 (dd, J_1=5.1 Hz, J_2=1.2 Hz, 1H). HRMS (ESI+): *m/z* calcd for $[M + H]^+$ 264.0689; found 264.0682.

4.3.27. Methyl 5-cyano-2-oxo-5-(thiophen-3-yl)cyclohexane-1-carboxylate (25)

Synthesized from 2-(thiophen-3-yl)acetonitrile (9.98 mL, 75.0 mmol, 1.0 equiv), methyl acrylate (34.00 mL, 375.2 mmol, 5.0 equiv) and benzyltrimethylammonium hydroxide (13.20 mL, 75.0 mmol, 1.0 equiv.) via general procedure A and potassium *tert*-butoxide (13.69 g, 122.0 mmol, 2 equiv) via general procedure B. The product was used without further purification. Yield: 62% (12.40 g); pale yellow solid. ^{1}H NMR (400 MHz, DMSO-d_6): δ 2.17–2.27 (m, 1H), 2.29–2.37 (m, 1H), 2.42–2.48 (m, 1H), 2.55–2.65 (m, 2H), 2.71 (dd, $J = 15.8$, 1.0 Hz, 1H), 2.94 (d, $J = 15.8$ Hz, 1H), 3.75 (s, 3H), 7.31 (dd, J_1=5.0 Hz, $J_2 = 1.5$ Hz, 1H), 7.63 (dd, J_1=2.9 Hz, $J_2 = 1.5$ Hz, 1H), 7.65 (dd, $J_1 = 5.0$ Hz, J_2 = 3.0 Hz, 1H). HRMS (ESI+): *m/z* calcd for $[M + H]^+$ 264.0689; found 264.0682.

4.3.28. 4-Oxo-1-(thiophen-2-yl)cyclohexane-1-carbonitrile (26)

Synthesized from **24** (12.64 g, 48.0 mmol, 1.0 equiv), 10% sulfuric acid (175 mL) and glacial acetic acid (385 mL) via general procedure C. Column chromatography, EtOAc/*n*-hexane = 1/3 (v/v). Yield: 50% (4.90 g); pale yellow solid. ^{1}H NMR (400 MHz, $CDCl_3$): δ 2.31 (td, J_1 = 13.5 Hz, J_2 = 4.3 Hz, 2H), 2.52–2.61 (m, 2H), 2.61–2.69 (m, 2H), 2.80–2.92 (m, 2H), 7.03 (dd, J_1=5.1 Hz, J_2 = 3.6 Hz, 1H), 7.20 (dd, J_1=3.6 Hz, J_2 = 1.2 Hz, 1H), 7.33 (dd, J_1=5.1 Hz, J_2 = 1.2 Hz, 1H). HRMS (ESI+): *m/z* calcd for $[M + H]^+$ 206.0634; found 206.0629.

4.3.29. 4-Oxo-1-(thiophen-3-yl)cyclohexane-1-carbonitrile (27)

Synthesized from **25** (12.40 g, 47.0 mmol, 1.0 equiv), 10% sulfuric acid (170 mL) and glacial acetic acid (380 mL) via general procedure C. Column chromatography, EtOAc/*n*-hexane = 1/3 (v/v). Yield: 62% (6.00 g); pale yellow solid. ^{1}H NMR (400 MHz, $CDCl_3$): δ 2.20–2.31 (m, 2H), 2.51–2.61 (m, 4H), 2.80–2.93 (m, 2H), 7.16 (dd, J_1=5.1 Hz, J_2=1.5 Hz, 1H), 7.36 (dd, J_1=3.0 Hz, J_2=1.5 Hz, 1H), 7.42 (dd, J_1=5.1 Hz, J_2=3.0 Hz, 1H). HRMS (ESI+): *m/z* calcd for $[M + H]^+$ 206.0634; found 260.0628.

4.3.30. 8-(Thiophen-2-yl)-1,4-dioxaspiro[4.5]decane-8-carbonitrile (28)

Synthesized from **26** (4.93 g, 24.0 mmol, 1.0 equiv), ethane-1,2-diol (13.4 mL, 240.0 mmol, 10.0 equiv) and PTSA (86.10 mg, 0.5 mmol, 0.02 equiv.) via general procedure D. Column chromatography, EtOAc/*n*-hexane = 1/3 (v/v). Yield: 98% (5.90 g); white solid. ^{1}H NMR (400 MHz, $CDCl_3$): δ 1.82–1.90 (m, 2H), 2.06 (td, J_1=13.4 Hz, J_2=4.0 Hz, 2H), 2.19 (td, J_1=13.2 Hz, J_2=3.5 Hz, 2H), 2.28–2.38 (m, 2H), 3.93–3.98 (m, 2H), 3.98–4.03 (m, 2H), 6.99 (dd, J_1=5.1 Hz, J_2=3.6 Hz, 1H), 7.15 (dd, J_1=3.6 Hz, J_2=1.2 Hz, 1H), 7.27 (dd, J_1=5.2 Hz, J_2=1.3 Hz, 1H). HRMS (ESI+): *m/z* calcd for $[M + H]^+$ 250.0896; found 250.0890.

4.3.31. 8-(Thiophen-3-yl)-1,4-dioxaspiro[4.5]decane-8-carbonitrile (29)

Synthesized from **27** (5.95 g, 29.0 mmol, 1.0 equiv), ethane-1,2-diol (16.2 mL, 290.0 mmol, 10.0 equiv) and PTSA (86.10 mg, 0.5 mmol, 0.02 equiv.) via general procedure D. Column chromatography, EtOAc/*n*-hexane = 1/3 (v/v). Yield: 96% (6.70 g); white solid. ^{1}H NMR (400 MHz, $CDCl_3$): δ 1.80–1.89 (m, 2H), 2.01–2.18 (m, 4H), 2.18–2.26 (m, 2H), 3.93–3.98 (m, 2H), 3.98–4.03 (m, 2H), 7.15 (dd, J_1=5.1 Hz, J_2=1.5 Hz, 1H), 7.30 (dd, J_1=3.0 Hz, J_2=1.5 Hz, 1H), 7.35 (dd, J_1=5.1 Hz, J_2=3.0 Hz, 1H). HRMS (ESI+): *m/z* calcd for $[M + H]^+$ 250.0896; found 250.0890.

4.3.32. (8-(Thiophen-2-yl)-1,4-dioxaspiro[4.5]decan-8-yl)methanamine (30)

Synthesized from **28** (5.90 g, 23.5 mmol, 1.0 equiv) and $LiAlH_4$ (1.78 g, 47.0 mmol, 2.0 equiv) via general procedure E. The product was used without further purification. Yield: 97% (5.80 g); pale yellow oil. Yield: 97% (5.8 g); oil. ^{1}H NMR (400 MHz, $CDCl_3$): δ 0.95 (brs, 2H), 1.63–1.74 (m, 4H), 1.75–1.85 (m, 2H), 2.10–2.18 (m, 2H), 2.72 (s, 2H), 3.89–3.98 (m, 4H), 6.86 (dd, J_1=3.5 Hz, J_2=1.1 Hz, 1H), 6.97 (dd, J_1=5.1 Hz, J_2=3.5 Hz, 1H), 7.21 (dd, J_1=5.1 Hz, J_2=1.1 Hz, 1H). HRMS (ESI+): *m/z* calcd for $[M + H]^+$ 254.1209; found 254.1201.

4.3.33. (8-(Thiophen-3-yl)-1,4-dioxaspiro[4.5]decan-8-yl)methanamine (31)

Synthesized from **29** (6.70 g, 27.0 mmol, 1.0 equiv) and $LiAlH_4$ (2.05 g, 54.0 mmol, 2.0 equiv) via general procedure E. The product was used without further purification. Yield: 96% (6.60 g); pale yellow oil. ^{1}H NMR (400 MHz, $CDCl_3$): δ 0.96 (brs, 2H), 1.55–1.70 (m, 4H), 1.70–1.79 (m, 2H), 2.09–2.16 (m, 2H), 2.68 (s, 2H), 3.88–3.97 (m, 4H), 7.01 (dd, J_1=5.0 Hz, J_2=1.4 Hz, 1H), 7.03 (dd, J_1=3.0 Hz, J_2=1.4 Hz, 1H), 7.31 (dd, J_1=5.0 Hz, J_2=3.0 Hz, 1H). HRMS (ESI+): *m/z* calcd for $[M + H]^+$ 254.1209; found 254.1201.

4.3.34. 2-Methoxy-N-((8-(thiophen-2-yl)-1,4-dioxaspiro[4.5]decan-8-yl) methyl)benzamide (32)

Synthesized from **30** (5.80 g, 22.8 mmol, 1.0 equiv), 2-methoxybenzoyl chloride (3.89 g, 22.8 mmol, 1 equiv) and Et_3N (9.5 mL, 68.4 mmol, 3.0 equiv.) via general procedure F. Column chromatography, EtOAc/*n*-hexane = 1/1 (v/v). Yield: 95% (8.40 g); white solid. ^{1}H NMR (400 MHz, $CDCl_3$): δ 1.65–1.80 (m, 4H), 1.95–2.05 (m, 2H), 2.12–2.20 (m, 2H), 3.68 (d, J = 6.0 Hz, 2H), 3.73 (s, 3H), 3.87–3.98 (m, 4H), 6.90 (d, J = 7.8 Hz, 1H), 6.95 (dd, J_1=3.5 Hz, J_2=1.1 Hz, 1H), 7.03 (ddd, J_1=9.5 Hz, J_2=6.6 Hz, J_3=2.2 Hz, 2H), 7.27 (dd, J_1=5.1 Hz, J_2=1.0 Hz, 1H), 7.40 (ddd, J_1=8.3 Hz, J_2=7.3 Hz, J_3=1.9 Hz, 1H), 7.77 (t, J = 4.9 Hz, 1H), 8.20 (dd, J_1=7.8 Hz, J_2=1.9 Hz, 1H). HRMS (ESI+): *m/z* calcd for $[M + H]^+$ 388.1577; found 388.1565.

4.3.35. 2-Methoxy-N-((8-(thiophen-3-yl)-1,4-dioxaspiro[4.5]decan-8-yl) methyl)benzamide (33)

Synthesized from **31** (6.60 g, 26.0 mmol, 1.0 equiv), 2-methoxybenzoyl chloride (4.40 g, 26.0 mmol, 1 equiv) and Et_3N (10.9 mL, 78.0 mmol, 3.0 equiv.) via general procedure F. Column chromatography, EtOAc/*n*-hexane = 1/1 (v/v). Yield: 89% (8.90 g); white solid. ^{1}H NMR (400 MHz, $CDCl_3$): δ 2.07–2.18 (m, 2H), 2.30–2.44 (m, 4H), 2.45–2.55 (m, 2H), 3.76 (s, 3H), 3.77 (d, J = 6.3 Hz, 2H), 3.85–3.96 (m, 4H), 6.92 (d, J = 8.4 Hz, 1H), 7.07 (td, J = 7.9, 1.0 Hz, 1H), 7.18 (dd, J = 5.0, 1.4 Hz, 1H), 7.21 (dd, J = 2.9, 1.4 Hz, 1H), 7.40–7.48 (m, 2H), 7.75 (brs, 1H), 8.20 (dd, J = 7.8, 1.8 Hz, 1H). HRMS (ESI+): *m/z* calcd for $[M + H]^+$ 388.1577; found 388.1565.

4.4. PBMC

4.4.1. Isolation and activation

PBMC were obtained by FICOLL-gradient purification (Lympholye - H Cedarlane) and have been treated with red blood cell lysis buffer [38]. Purified PBMC were seeded at 1.5 × 10^6 cells/mL in RPMI 10% heat inactivated serum supplemented with L-Glutamine [2 mM] in presence or absence of the different tested drugs, and treated with 240 ng/mL of phytohemagglutinin-L (PHA-L) (Merck) for 5 days before patch clamp recordings, counts and FACS analysis. The composition of the purified PBMC has been analyzed after 5 days of PHA stimulation and resulted composed mostly (~90%) by $CD3^+$ T-lymphocytes.

4.4.2. Patch-clamp recordings

Cells were directly transferred on 35 mm petri dishes containing the following solution (in mM): 130 NaCl, 5 KCl, 2 $CaCl_2$, 2 $MgCl_2$, 10 HEPES, 5 D-glucose (EK = −83 mV), pH of 7.4. The internal pipette solution for potassium currents measurement contained (in mM): 140 potassium fluoride, 1 $CaCl_2$, 2 $MgCl_2$, 10 Hepes–NaOH, 11 EGTA, pH 7.2. The patch pipettes were pulled from borosilicate glass capillary tubes, their resistance was 6–8 MΩ and their capacitances were manually compensated up to 90–95% after the reaching of a stable gigaseal. Experimental protocols and data acquisition have been performed with the Multiclamp 700A amplifier, digitized with Digidata 1322A DAC and pCLAMP 9.2 software (Molecular Devices, Sunnyvale, California, USA) has been used for data analysis. The outward potassium currents were digitized with a 25 KHz sampling rate and a 3 KHz low-pass filtered. Cells' identification and patch has been performed at 40x magnification with a Nikon Eclipse TE300 microscope (Nikon Instruments Inc.). In order to perform the electrophysiological recordings specifically on the activated cells, we visually chose the cells that showed a larger size compared the others present in the Petri dish as previously reported [39]. In accordance, the cells we selected showed potassium currents, in control conditions, of an amplitude comparable to those observed by other authors [40], while the cells of a smaller size showed current amplitudes of less than 500–600 pA. We consequently discarded all the cells having currents lower than or equal to 500–600 pA, classifying them as non-activated cells. Potassium currents were evoked by using a double sweep protocol with an intersweep interval of 30 s: the first sweep, starting from holding potential of 0 mV (30 s), was followed by a pulse to 60 mV and used to measure leak current, the second sweep, with holding potential of −80 mV, was followed by a pulse to 60 mV and was used to measure the potassium current. Net traces (leak-subtracted) were obtained by subtracting the one recorded in the first sweep from the current recorded in the second one. TRAM-34, a selective inhibitor of $K_{Ca}3.1$[33], was used respectively as reference drug. The same recording protocol was then performed both in control conditions and with increasing doses of compounds (0.05, 0.1, 0.5, 5, 50 nM, 5 and 50 μM) in order to evaluate the dose-response curves. The leak current was then subtracted from the evoked potassium current and the measured peak was normalized to the control value prior to evaluate the curve.

4.4.3. Intracellular Ca^{2+} measurement on PBMCs

Purified PBMC activated with PHA for 5 days have been treated with the different tested drugs [5 μM] for 2h, then have been detached from the plate with a scraper and incubated in RPMI containing 10% heat inactivated bovine calf serum (HyClone) and supplemented with 2 mM L-glutamine, supplemented with the Fluo-4 Ca^{2+} probe (Invitrogen) [2 μM] and anti CD3-APC (SK7 BD 1:100) at 37 °C for 1 h protected from light. Following washing with complete RPMI medium to remove residual dye, PBMC have been resuspended in 200 μL RPMI containing 10% heat inactivated bovine calf serum (HyClone) and supplemented with 2 mM L-glutamine, supplemented with the tested drugs [5 μM] at 37 °C for 30 min before acquisition with a CyotFLEX cytometer (Beckman Coulter).

4.4.4. Image collection and cell cycle analysis

Purified PBMC have been activated with PHA and treated with the different tested drugs [30 μM] in RPMI containing 10% heat inactivated bovine calf serum (HyClone) and supplemented with 2 mM L-glutamine for 5 days.

On day 5 the images of the wells containing the activated PBMC

treated with the different drugs in a 24 well plate were acquired for the evaluation of the number of colonies. The images were acquired, after removal of the culture media, with a bright field microscope (EVOS XL Core Imaging System, Advanced Microscopy Group (AMG) BOTHELL, WA 98021 USA) at the magnification of 2×. Colony counting was subsequently performed offline manually using the ImageJ software [41].

On day 5, after the image acquisition, the flow cytometry cell cycle analysis by quantitation of DNA content has been performed. 200 μL of a solution composed of 50 μg/mL propidium iodide (PI, Sigma Aldrich P4864), 0.1% (w/v) trisodium citrate, 0.1% NP40 were added directly into the wells containing the activated PBMC in the different experimental conditions. Cells were then detached from the plate with a scraper and incubated for 1 h at 4 °C protected from light before being analyzed with CyotFLEX cytometer (Beckman Coulter).

4.4.5. Statistics

Parametric tests were used for statistical analysis. Paired *t*-test was performed for electrophysiological analysis, while unpaired *t*-test was used for Ca^{2+}, n. CFU and cell cycle analysis. Data are reported as mean ± SEM. The normality of data distribution was checked with Kolmogorov–Smirnov test. Statistical analysis was performed using Prism 6 software (GraphPad Software, San Diego, CA, USA). All statistical tests were two tailed with a significance level of 0.05.

4.5. Xenopus laevis oocytes

4.5.1. Collection

Stage V–VI oocytes [26] were isolated by partial ovariectomy from *Xenopus laevis* frogs (African clawed frogs). Mature female frogs were purchased from CRB Xénopes (Rennes, France) and were housed in the Aquatic Facility (KU Leuven) in compliance with the regulations of the European Union (EU) concerning the welfare of laboratory animals as declared in Directive 2010/63/EU. The use of *Xenopus laevis* was approved by the Animal Ethics Committee of the KU Leuven (Project nr. P186/2019). After anaesthetizing the frogs by a 15-min submersion in 0.1% tricaine methanesulfonate (amino benzoic acid ethyl ester; Merck, Kenilworth, NJ, USA), pH 7.0, the oocytes were collected. The isolated oocytes were then washed with a 1.5 mg/mL collagenase solution for 2 h to remove the follicle layer.

4.5.2. Injection

Ion channels (K_V1.x1) [26] were expressed in *Xenopus laevis* oocytes by linearization of the plasmids and subsequent in vitro transcription using a commercial T7 or SP6 mMESSAGE mMACHINE transcription kit (Ambion, Carlsbad, California, USA). Defolliculated *Xenopus* oocytes were then injected with 20–50 nL of the cRNA at a concentration of 1 ng/nL using a micro-injector (Drummond Scientific1, Broomall, PA, USA). The oocytes were incubated in a solution containing (in mM): NaCl, 96; KCl, 2; $CaCl_2$, 1.8; $MgCl_2$, 2 and HEPES, 5 (pH 7.5), supplemented with 50 mg/L gentamycin sulfate and 90 mg/L theophylline. After *ex vivo* translation, the ion channels were correctly inserted in the cell membrane of the oocytes.

4.5.3. Compound solutions, and electrophysiological recordings

Two-electrode voltage-clamp recordings [26,27] were performed at room temperature (18–22 °C) using a Geneclamp 500 amplifier (Molecular Devices, San Jose, CA, USA) and pClamp data acquisition (Axon Instruments, Union City, CA, USA) and using an integrated digital TEVC amplifier controlled by HiClamp, an automated Voltage-Clamp Screening System (Multi Channel Systems MCS GmbH, Reutlingen, Germany). Whole-cell currents from oocytes were recorded 1–4 days after injection. The bath solution composition was ND96 (in mM): NaCl, 96; KCl, 2; $CaCl_2$, 1.8; $MgCl_2$, 2 and HEPES, 5 (pH 7.5). Voltage and current electrodes were filled with a 3 M solution of KCl in H_2O. Resistances of both electrodes were kept between 0.5 and 1.5 MΩ. The elicited K_V1.x currents were filtered at 0.5 kHz and sampled at 2 kHz using a four-pole low-pass Bessel filter. Leak subtraction was performed using a P/4 protocol.

For the electrophysiological analysis of the compounds, a number of protocols were applied from a holding potential of −90 mV. Currents for K_V1.x were evoked by 1 s depolarizing pulses either to 0 mV or to a range of voltage steps between −80 mV and +40 mV. For the analysis of the data, only the inhibition at the 0 mV step was used. The concentration dependency of all compounds was assessed by measuring the current inhibition in the presence of increasing compound concentrations. To this end, a stock solution of the compounds was prepared in 100% DMSO for the sake of solubility. From this stock solution, adequate dilutions with a maximum of 0.5% DMSO were made for testing. The data of the concentration-response curves were fitted with the Hill equation: $y = 100/\{1 + (IC_{50}/[\text{compound}])^h\}$, where y is the amplitude of the compound-induced effect, IC_{50} is the compound concentration at half-maximal efficacy, [compound] is the compound concentration, and h is the Hill coefficient.

4.5.4. Statistical analysis

All electrophysiological data are presented as means ± S.E.M of n ≥ three independent experiments unless otherwise indicated. All data were analyzed using pClamp Clampfit 10.4 (Molecular Devices, Downingtown, PA, USA), OriginPro 9 (Originlab, Northampton, MA, USA), GraphPad Prism 8 software (GraphPad Software, Inc., San Diego, CA, USA) and DataMining (Multi Channel Systems MCS GmbH, Reutlingen, Germany). The Dunnett test and one-way ANOVA were performed to calculate the significance of the induced inhibition compared to the control.

4.6. Ltk⁻ cells

4.6.1. Cell culture, and transfection

Ltk⁻ cells [27] were cultured in Dulbecco's Modified Eagle Medium (DMEM) supplemented with 10% horse serum and 1% penicillin/streptomycin (Invitrogen, Waltham, CA, USA). Human K_V1.3 channels were transiently expressed in these Ltk⁻ cells by transfecting subconfluent 60 × 15 mm cell culture dishes (Corning, NY, USA) with 1–1.5 μg plasmid DNA containing the hKv1.3 sequence (KCNA3) using lipofectamine 2000 (Thermo Fisher Scientific, Waltham, MA, USA), according to the manufacturer's protocol. The coding sequence of hKv1.3 was cloned in a pEGFP plasmid without removing the stop codon (i.e., eGFP was not transcribed). Therefore, during transfection 0.5 μg of pEGFP plasmid (expressing eGFP) was added as transfection marker. Cells were collected 24 h post-transfection using a 0.05% trypsin-EDTA solution (Thermo Fisher Scientific, Waltham, MA, USA) and transferred to the recording chamber mounted on the stage of an inverted Nikon Eclipse TE2000 fluorescence microscope (Nikon, Minato, Japan). The compounds were dissolved in 100% DMSO and stock solutions were stored at −20 °C. Before use, the stock concentrations were diluted with extracellular recording solution to appropriate concentrations, making sure that the final DMSO concentration never exceeded 0.1%. As a vehicle control a 0.1% DMSO solution was prepared.

4.6.2. Compound solutions, and electrophysiological recordings

All recordings were conducted at room temperature (20–23 °C) in the whole-cell configuration using an axopatch 200b amplifier (Molecular Devices, San Jose, CA, USA). Applied voltage pulse protocols and current recordings were controlled with pClamp 10 software and digitized using an axon digidata 1440 (Molecular Devices, San Jose, CA, USA). The cells in the recording chamber were continuously superfused with an extracellular solution (containing in mM): NaCl 145, KCl 4, $MgCl_2$ 1, $CaCl_2$ 1.8, HEPES 10, and D-glucose 10 (adjusted to pH 7.35 with NaOH). Patch pipettes were pulled from borosilicate glass (World Precision Instruments, Sarasota, FL, USA), using a P-2000 puller (Sutter Instruments, Novato, CA, USA), with resistances ranging from 1.5 to 2 MΩ. These pipettes were backfilled with an intracellular solution

(containing in mM): KCl 110, K_2ATP 5, $MgCl_2$ 2, HEPES 10, and K_4BAPTA 5 (adjusted to pH 7.2 with KOH). Junction potentials were zeroed with the filled pipette in the extracellular solution of the recording chamber. A series resistance compensation of 80% was employed. Recordings were passed through a 5 kHz low-pass filter while being sampled at 10 kHz. A single step from holding potential (−80 mV) to +40 mV was utilized to monitor $hK_V1.3$ current inhibition. The pulse duration was 200 ms with an interpulse interval of 15 s. Different concentrations of the compounds were independently added to the recording chamber in the vicinity of the investigated cell using a pressurized fast-perfusion system (custom built with electro-fluidic valves from the Lee Company, Westbrook, CT, USA).

4.6.3. Statistical analysis

The data was analyzed with pClamp 10 software (Molecular Devices, San Jose, CA, USA), and the dose-response curves shown were made using Sigmaplot 11.0 (Systat software, Palo Alto, CA USA). Data was excluded when the estimated voltage error exceeded 5 mV after series resistance compensation. Dose-response curves were obtained by plotting y, the normalized current, as a function of compound concentration. Results are expressed as mean ± SEM, with n being the number of cells analyzed. IC_{50} values were determined by fitting the Hill equation to the dose-response curve.

4.7. Thermodynamic solubility

Thermodynamic solubility was determined as a concentration of a saturated solution in equilibrium (37 °C) in phosphate buffered saline (pH = 7.4) using HPLC method. For the phosphate-buffered saline (PBS), 2.38 g of disodium hydrogen phosphate dodecahydrate, 0.19 g of potassium dihydrogen phosphate, and 8.0 g of sodium chloride were added to distilled water (900 mL) and the solution was mixed overnight. The next day, it was diluted to 1000 mL with the same solvent and the pH was adjusted to 7.4. Samples (dry powders) were prepared by weighing the exact mass of compounds (about 1 mg) and then adding the appropriate volume of PBS to reach the final concentration of approx. 1 mg/mL. The samples were shaken (60 rpm) at 37 °C for 24 h using orbital shaking incubator. After 24 h they were centrifuged at 18000 rpm for 10 min. Samples for injection were prepared by diluting (1:2 or 1:10) the supernatant with a 1:1 mixture of 0.1% TFA [v/v] in water and MeCN. For the 7-point calibration curves concentrated stock solutions of the compounds were prepared at concentrations of 10 mM and 0.5 mM in DMSO, which were diluted with a 1:1 mixture of 0.1% TFA [v/v] in water and MeCN to a final concentration of 100 μM; 70 μM; 50 μM; 30 μM; 15 μM; 5 μM and 1 μM. Quality control (QC) samples were diluted from stock solutions with a 1:1 mixture of 0.1% TFA [v/v] in water and MeCN to final concentrations of 60 μM, 20 μM, and 2 μM. Analytical reversed-phase UPLC analyses were performed using a modular system (Thermo Scientific Dionex UltiMate 3000 modular system; Thermo Fisher Scientific Inc., MA, USA). Method: Waters Acquity UPLC® HSS C18 SB column (2.1 × 50 mm, 1.8 μm), T = 40 °C; injection volume = 5 μL; flow rate = 0.4 mL/min; detector λ = 290 nm; mobile phase A (0.1% TFA [v/v] in water), mobile phase B (MeCN). Gradient: 0–2 min, 10% B; 2–10 min, 10%–90% B; 10–12 min, 90% B. Results are given in μM as an average value of two independent experiments.

4.8. Stability

The method used for assessing aqueous stability was as followed: Waters Acquity UPLC® BEH C18 column (2.1 × 50 mm, 1.7 μm) thermostated at 40 °C; injection volume, 10 μL; flow rate, 0.4 mL/min; detector λ, 280 nm; mobile phase A: H_2O/MeCN/MeOH/TFA 900/80/20/1 (v/v); mobile phase B: MeCN/MeOH/TFA 800/200/1 (v/v). Method: 0–5 min, 20%–100% B; 5–6 min, 100% B; 6–6.1 min, 100%–20% B; 6.1–8 min, 20% B. A 10 mM stock solution of the compound *trans*-**18** was prepared in DMSO. For the stability 1590 μL of PBS buffer (pH = 7.4), 400 μL of MeCN, and 10 μL of the compound *trans*-**18** stock solution were mixed in microcentrifuge tubes. The solution was thoroughly mixed and filtered using a 0.20 μm filter into an HPLC vial, resulting in a final concentration of 50 μM for the compound *trans*-**18**, with 20% MeCN and 0.5% DMSO in PBS buffer. The solution was immediately injected and subsequent injections were performed at 4-h intervals for the first 24 h. Afterwards, injections were carried out at 8-h intervals while the solution was incubated at 37 °C. The experiment was conducted in triplicates, and the resulting analyte AUCs were plotted against time.

Author contributions

The manuscript was written through contributions of all authors. All authors have given approval to the final version of the manuscript.

Notes

The authors declare no competing financial interest.

Declaration of competing interest

The authors declare that they have no known competing financial interests or personal relationships that could have appeared to influence the work reported in this paper.

Data availability

No data was used for the research described in the article.

Acknowledgment

This research was funded by Slovenian Research Agency (ARRS) grant numbers J1-9192, N1-0098, P1-0208 and CELSA project. The work has also received funding from the Max-Planck Society and from the European Union through Horizon 2020 research and innovation programme under the Marie Skłodowska-Curie grant agreement No. 813834-PHIONIC-H2020-MSCA-ITN-2018. This study was supported by grants GOE7120 N, GOC2319 N, and GOA4919 N from the F.W.O. Vlaanderen, awarded to J.T. and S.P. was supported by KU Leuven funding (PDM/19/164) and F.W.O. Vlaanderen grant 12W7822 N.

Appendix A. Supplementary data

Supplementary data to this article can be found online at https://doi.org/10.1016/j.ejmech.2023.115561.

Abbreviations

CCR2	CC chemokine receptor 2
CCL2	CC chemokine ligand 2
CCR5	CC chemokine receptor 5
TLC	thin layer chromatography
PHA	phytohemagglutinin
PBMC	peripheral blood mononuclear cells
TD	thermodynamic
T_{CM}	central memory T-cells
T_{EM}	effector memory T-cell
SCID	severe combined immunodeficiency
THF	tetrahydrofuran
PTSA	*p*-toluenesulfonic acid
DMF	*N,N*-dimethylformamide,
TCR	T-cell receptor
NFAT	nuclear factor of activated T-cells
CFU	colony-forming units
B-CLL	B-cell chronic lymphocytic leukemia

ALL	T-cell acute lymphoblastic leukemia
TFA	trifluoroacetic acid
MeCN	acetonitrile,
MeOH	methanol
DCM	dichloromethane
EtOAc	ethylacetate

References

[1] S. Feske, E.Y. Skolnik, M. Prakriya, Ion channels and transporters in lymphocyte function and immunity, Nat. Rev. Immunol. 12 (7) (2012) 532–547.

[2] M.D. Cahalan, K.G. Chandy, The functional network of ion channels in T lymphocytes, Immunol. Rev. 231 (1) (2009) 59–87, https://doi.org/10.1111/j.1600-065X.2009.00816.x.

[3] J. Wang, M. Xiang, Targeting potassium channels $K_V1.3$ and $K_{Ca}3.1$: routes to selective immunomodulators in autoimmune disorder treatment? Pharmacotherapy 33 (5) (2013) 515–528, https://doi.org/10.1002/phar.1236.

[4] P.G. Hogan, R.S. Lewis, A. Rao, Molecular basis of calcium signaling in lymphocytes: STIM and ORAI, Annu. Rev. Immunol. 28 (2010) 491–533, https://doi.org/10.1146/annurev.immunol.021908.132550.

[5] S. Feske, H. Wulff, E.Y. Skolnik, Ion channels in innate and adaptive immunity, Annu. Rev. Immunol. 33 (2015) 291–353, https://doi.org/10.1146/annurev-immunol-032414-112212.

[6] M.D. Cahalan, K.G. Chandy, T.E. DeCoursey, S. Gupta, A voltage-gated potassium channel in human T lymphocytes, J. Physiol. 358 (1985) 197–237, https://doi.org/10.1113/jphysiol.1985.sp015548.

[7] I.G. Ishida, G.E. Rangel-Yescas, J. Carrasco-Zanini, L.D. Islas, Voltage-dependent gating and gating charge measurements in the $K_V1.2$ potassium channel, J. Gen. Physiol. 145 (4) (2015) 345–358, https://doi.org/10.1085/jgp.201411300.

[8] X.M. Xia, B. Fakler, A. Rivard, G. Wayman, T. Johnson-Pais, J.E. Keen, T. Ishii, B. Hirschberg, C.T. Bond, S. Lutsenko, J. Maylie, J.P. Adelman, Mechanism of calcium gating in small-conductance calcium-activated potassium channels, Nature 395 (6701) (1998) 503–507, https://doi.org/10.1038/26758.

[9] E.Y. Chiang, T. Li, S. Jeet, I. Peng, J. Zhang, W.P. Lee, J. DeVoss, P. Caplazi, J. Chen, S. Warming, D.H. Hackos, S. Mukund, C.M. Koth, J.L. Grogan, Potassium channels $K_V1.3$ and $K_{Ca}3.1$ cooperatively and compensatorily regulate antigen-specific memory T cell functions, Nat. Commun. 8 (2017), 14644, https://doi.org/10.1038/ncomms14644.

[10] C. Beeton, H. Wulff, J. Barbaria, O. Clot-Faybesse, M. Pennington, D. Bernard, M. D. Cahalan, K.G. Chandy, E. Béraud, Selective blockade of T lymphocyte K(+) channels ameliorates experimental autoimmune encephalomyelitis, a model for multiple sclerosis, Proc. Natl. Acad. Sci. U. S. A. 98 (24) (2001) 13942–13947, https://doi.org/10.1073/pnas.241497298.

[11] R.J. Leonard, M.L. Garcia, R.S. Slaughter, J.P. Reuben, Selective blockers of voltage-gated K^+ channels depolarize human T lymphocytes: mechanism of the antiproliferative effect of charybdotoxin, Proc. Natl. Acad. Sci. U. S. A. 89 (21) (1992) 10094–10098, https://doi.org/10.1073/pnas.89.21.10094.

[12] S. Srivastava, K. Ko, P. Choudhury, Z. Li, A.K. Johnson, V. Nadkarni, D. Unutmaz, W.A. Coetzee, E.Y. Skolnik, Phosphatidylinositol-3 phosphatase myotubularin-related protein 6 negatively regulates CD4 T cells, Mol. Cell Biol. 26 (15) (2006) 5595–5602, https://doi.org/10.1128/MCB.00352-06.

[13] L. Leanza, L. Trentin, K.A. Becker, F. Frezzato, M. Zoratti, G. Semenzato, E. Gulbins, I. Szabo, Clofazimine, psora-4 and PAP-1, inhibitors of the potassium channel $K_V1.3$, as a new and selective therapeutic strategy in chronic lymphocytic leukemia, Leukemia 27 (8) (2013) 1782–1785, https://doi.org/10.1038/leu.2013.56.

[14] T.E. DeCoursey, K.G. Chandy, S. Gupta, M.D. Cahalan, Voltage-gated K^+ channels in human T lymphocytes: a role in mitogenesis? Nature 307 (5950) (1984) 465–468, https://doi.org/10.1038/307465a0.

[15] A. Magi, M. Masselli, C. Sala, A. Guerriero, P. Laise, B. Puccini, L. Rigacci, C. Breschi, O. Crociani, S. Pillozzi, A. Arcangeli, The ion channels and transporters gene expression profile indicates a shift in excitability and metabolisms during malignant progression of follicular lymphoma, Sci. Rep. 9 (1) (2019) 8586, https://doi.org/10.1038/s41598-019-44661-x.

[16] C. Sala, A. Arcangeli, Reduced bcr signaling and a metabolic shift accompanies malignant progression of follicular lymphoma: a lesson from transcriptomics, Arch. Cancer Biol. Ther. 1 (2) (2020) 31–36, https://doi.org/10.33696/cancerbiology.1.007.

[17] H. Wulff, M. Pennington, Targeting effector memory T-cells with Kv1.3 blockers, Curr. Opin. Drug Discov. Dev 10 (4) (2007) 438–445.

[18] Š. Gubič, L.A. Hendrickx, Ž. Toplak, M. Sterle, S. Peigneur, T. Tomašič, L.A. Pardo, J. Tytgat, A. Zega, L. Peterlin Mašič, Discovery of $K_V1.3$ ion channel inhibitors: medicinal chemistry approaches and challenges, Med. Res. Rev. 41 (4) (2021) 2423–2473, https://doi.org/10.1002/med.21800.

[19] R. Chen, A. Robinson, D. Gordon, S.-H. Chung, Modeling the binding of three toxins to the voltage-gated potassium channel ($K_V1.3$), Biophys. J. 101 (11) (2011) 2652–2660, https://doi.org/10.1016/j.bpj.2011.10.029.

[20] A. Schmitz, A. Sankaranarayanan, P. Azam, K. Schmidt-Lassen, D. Homerick, W. Hänsel, H. Wulff, Design of PAP-1, a selective small molecule $K_V1.3$ blocker, for the suppression of effector memory T cells in autoimmune diseases, Mol. Pharmacol. 68 (5) (2005) 1254–1270, https://doi.org/10.1124/mol.105.015669.

[21] S. Kundu-Raychaudhuri, Y.-J. Chen, H. Wulff, S.P. Raychaudhuri, $K_V1.3$ in psoriatic disease: PAP-1, a small molecule inhibitor of $K_V1.3$ is effective in the SCID mouse psoriasis–xenograft model, J. Autoimmun. 55 (2014) 63–72, https://doi.org/10.1016/j.jaut.2014.07.003.

[22] PAP-1 Datasheet. https://www.selleckchem.com/datasheet/pap-1-E037801-DataSheet.html. (Accessed 13 June 2022).

[23] R. Peruzzo, A. Mattarei, M. Azzolini, K.A. Becker-Flegler, M. Romio, G. Rigoni, A. Carrer, L. Biasutto, S. Parrasia, S. Kadow, A. Managò, A. Urbani, A. Rossa, G. Semenzato, M.E. Soriano, L. Trentin, S. Ahmad, M. Edwards, E. Gulbins, C. Paradisi, M. Zoratti, L. Leanza, I. Szabò, Insight into the mechanism of cytotoxicity of membrane-permeant psoralenic $K_V1.3$ channel inhibitors by chemical dissection of a novel member of the family, Redox Biol. 37 (2020), 101705, https://doi.org/10.1016/j.redox.2020.101705.

[24] J. Vennekamp, H. Wulff, C. Beeton, P.A. Calabresi, S. Grissmer, W. Hänsel, K. G. Chandy, Kv1.3-Blocking 5-phenylalkoxypsoralens: a new class of immunomodulators, Mol. Pharmacol. 65 (6) (2004) 1364–1374, https://doi.org/10.1124/mol.65.6.1364.

[25] W.A. Schmalhofer, J. Bao, O.B. McManus, B. Green, M. Matyskiela, D. Wunderler, R.M. Bugianesi, J.P. Felix, M. Hanner, A.-R. Linde-Arias, C.G. Ponte, L. Velasco, G. Koo, M.J. Staruch, S. Miao, W.H. Parsons, K. Rupprecht, R.S. Slaughter, G. J. Kaczorowski, M.L. Garcia, Identification of a new class of inhibitors of the voltage-gated potassium channel, $K_V1.3$, with immunosuppressant properties, Biochemistry 41 (24) (2002) 7781–7794, https://doi.org/10.1021/bi025722c.

[26] L.A. Hendrickx, V. Dobričić, Ž. Toplak, S. Peigneur, L. Peterlin Mašič, T. Tomašič, J. Tytgat, Design and characterization of a novel structural class of $K_V1.3$ inhibitors, Bioorg. Chem. 98 (2020), 103746, https://doi.org/10.1016/j.bioorg.2020.103746.

[27] Š. Gubič, L.A. Hendrickx, X. Shi, Ž. Toplak, Š. Možina, K.M. Van Theemsche, E. L. Pinheiro-Junior, S. Peigneur, A.J. Labro, L.A. Pardo, J. Tytgat, T. Tomašič, L. Peterlin Mašič, Design of new potent and selective thiophene-based $K_V1.3$ inhibitors and their potential for anticancer activity, Cancers 14 (11) (2022) 2595, https://doi.org/10.3390/cancers14112595.

[28] K.G. Chandy, R.S. Norton, Peptide blockers of $K_V1.3$ channels in T cells as therapeutics for autoimmune disease, Curr. Opin. Chem. Biol. 38 (2017) 97–107, https://doi.org/10.1016/j.cbpa.2017.02.015.

[29] Š. Gubič, L.A. Hendrickx, Ž. Toplak, M. Sterle, S. Peigneur, T. Tomašič, L.A. Pardo, J. Tytgat, A. Zega, L.P. Mašič, Discovery of KV 1.3 ion channel inhibitors: medicinal chemistry approaches and challenges, Med. Res. Rev. 41 (4) (2021) 2423–2473, https://doi.org/10.1002/med.21800.

[30] K.G. Chandy, H. Wulff, C. Beeton, M. Pennington, G.A. Gutman, M.D. Cahalan, K^+ channels as targets for specific immunomodulation, Trends Pharmacol. Sci. 25 (5) (2004) 280–289, https://doi.org/10.1016/j.tips.2004.03.010.

[31] A. Teisseyre, A. Palko-Labuz, K. Sroda-Pomianek, K. Michalak, Voltage-gated potassium channel $K_V1.3$ as a target in therapy of cancer, Front. Oncol. 9 (2019), https://doi.org/10.3389/fonc.2019.00933.

[32] S. Valle-Reyes, O. Dobrovinskaya, I. Pottosin, $K_V1.3$ current voltage dependence in lymphocytes is modulated by Co-culture with bone marrow-derived stromal cells: B and T cells respond differentially, Cell. Physiol. Biochem. Int. J. Exp. Cell. Physiol. Biochem. Pharmacol. 54 (5) (2020) 842–852, https://doi.org/10.33594/000000273.

[33] H. Wulff, M.J. Miller, W. Hansel, S. Grissmer, M.D. Cahalan, K.G. Chandy, Design of a potent and selective inhibitor of the intermediate-conductance Ca^{2+}-activated K^+ channel, IKCa1: a potential immunosuppressant, Proc. Natl. Acad. Sci. USA 97 (14) (2000) 8151–8156, https://doi.org/10.1073/pnas.97.14.8151.

[34] V.N. Uebele, S.K. England, A. ChaudHary, M.M. Tamkun, D.J. Snyders, Functional differences in Kv1.5 currents expressed in mammalian cell lines are due to the presence of endogenous Kvb2.1 subunits, J. Biol. Chem. 271 (5) (1996) 2406–2412.

[35] C. Beeton, H. Wulf, N.E. Standifer, K.G. Chandy, Kv1.3 channels are a therapeutic target for T cell-mediated autoimmune diseases, Proc. Natl. Acad. Sci. U.S.A. 103 (46) (2006) 17414–17419.

[36] M.D. Chalan, K.G. Chandy, The functional network of ion channels in T lymphocytes, Immunol. Rev. 231 (1) (2009) 59–87.

[37] I. Szabo, L. Trentin, V. Trimarco, G. Semenzato, L. Leanza, Biophysical characterization and expression analysis of Kv1.3 potassium channel in primary human leukemic B cells, Cell. Physiol. Biochem. 37 (3) (2015) 965–978, https://doi.org/10.1159/000430223.

[38] S. Panda, B. Ravindran, Isolation of human PBMCs, BIO-Protoc. 3 (3) (2013), https://doi.org/10.21769/BioProtoc.323.

[39] G. Panyi, Biophysical and pharmacological aspects of K^+ channels in T lymphocytes, Eur. Biophys. J. EBJ 34 (6) (2005) 515–529, https://doi.org/10.1007/s00249-005-0499-3.

[40] J. Vennekamp, H. Wulff, C. Beeton, P.A. Calabresi, S. Grissmer, W. Hänsel, K. G. Chandy, $K_V1.3$ -blocking 5-phenylalkoxypsoralens: a new class of immunomodulators, Mol. Pharmacol. 65 (6) (2004) 1364–1374, https://doi.org/10.1124/mol.65.6.1364.

[41] C.A. Schneider, W.S. Rasband, K.W. Eliceiri, NIH image to ImageJ: 25 Years of image analysis, Nat. Methods 9 (7) (2012) 671–675, https://doi.org/10.1038/nmeth.2089.